YALE PEABODY MUSEUM

JOURNAL OF MARINE RESEARCH

The *Journal of Marine Research,* one of the oldest journals in American marine science, published important peer-reviewed original research on a broad array of topics in physical, biological, and chemical oceanography vital to the academic oceanographic community in the long and rich tradition of the Sears Foundation for Marine Research at Yale University.

An archive of all issues from 1937 to 2021 (Volume 1–79) are available through EliScholar, a digital platform for scholarly publishing provided by Yale University Library at https://elischolar.library.yale.edu/.

Requests for permission to clear rights for use of this content should be directed to the authors, their estates, or other representatives. The *Journal of Marine Research* has no contact information beyond the affiliations listed in the published articles. We ask that you provide attribution to the *Journal of Marine Research.*

Yale University provides access to these materials for educational and research purposes only. Copyright or other proprietary rights to content contained in this document may be held by individuals or entities other than, or in addition to, Yale University. You are solely responsible for determining the ownership of the copyright, and for obtaining permission for your intended use. Yale University makes no warranty that your distribution, reproduction, or other use of these materials will not infringe the rights of third parties.

Signatures of stirring and mixing near the Gulf Stream front

by G. L. Hitchcock[1], T. Rossby[2], J. L. Lillibridge III[3], E. J. Lessard[4], E. R. Levine[5], D. N. Connors[5], K. Y. Børsheim[6], and M. Mork[7]

ABSTRACT

In October, 1986 the surface waters adjacent to the Gulf Stream front were surveyed with an undulating profiler to describe the finescale structure of the mixed layer. The profiler was a Seasoar equipped with a CTD and fluorometer. The survey first defined the structure of a cyclonic eddy which resembled frontal eddies of the South Atlantic Bight in sea surface temperature imagery. The Seasoar transects revealed, however, that the cyclonic eddy lacked a cold dome typically seen in frontal eddies. Farther downstream the Seasoar defined the structure of streamers of Gulf Stream and Shelf water wrapped about the southern edge of a warm-core ring. The streamers had lateral and along-axis dimensions on the order of ≈ 10 km and 100 km, respectively, and were bordered by narrow intrusive features. The temporal history of the streamers was described from SST imagery, and the surface flow derived from ship's drift vectors. CTD casts taken while following an isopycnal float provided a means to examine the structure of the intrusive features. Interleaving was evident at the boundaries of the streamers and intrusive features where high conductivity Cox numbers were concentrated, suggesting elevated microstructure activity. The Turner angle distribution, indicating either saltfingering or diffusive convection, did not correlate well with the Cox number distribution. This is interpreted as evidence that lateral, rather than diapycnal, mixing was the process mediating the exchange of properties at the boundaries of contrasting water types. In contrast to physical properties, the distribution of fluorescence showed relatively less structure in the surface layer between the ring and Gulf Stream front. In the surface layers of the two streamers the pigment and bacterial biomass, and the diatom species composition, were typical of Slope water communities. We hypothesize that small-scale mixing processes concentrated at the boundaries of the streamers were the mechanism by which Slope water plankton were seeded into streamers of different hydrographic origins. Presumably, high netplankton growth rates allowed the Slope water species to dominate the communities in the streamers.

1. Rosenstiel School of Marine and Atmospheric Sciences, University of Miami, Miami, Florida, 33149, U.S.A.
2. Graduate School of Oceanography, University of Rhode Island, Narranagansett, Rhode Island, 02882, U.S.A.
3. National Ocean Service, NOAA, Silver Springs, Maryland, 20910, U.S.A.
4. School of Oceanography, University of Washington, Seattle, Washington, 98195, U.S.A.
5. Code 8212, Naval Undersea Warfare Center, Newport, Rhode Island, 02841, U.S.A.
6. The Norwegian Institute of Technology, University of Trondheim, Trondheim, Norway.
7. Geofysik Institutt, Universitetet i Bergen, Bergen, Norway.

1. Introduction

One of the most persistent features in the northwestern Atlantic is the strong property front which extends along the cyclonic edge of the Gulf Stream. The front is defined by sharp gradients in salt, temperature, and dissolved oxygen which indicate there is limited exchange between the Slope Water and the Gulf Stream (Bower *et al.*, 1985). The Gulf Stream front also delineates a boundary between the subtropical plankton communities of the oligotrophic Gulf Stream-Sargasso Sea, and the temperate communities of the Slope water (e.g., Wishner and Allison, 1986). Several processes, however, contribute to the exchange of heat, salt and plankton across the Gulf Stream front. Large volumes of Gulf Stream and Slope waters, and their entrained plankton communities, are transferred between the contrasting water masses during the formation of warm- and cold-core rings (Olson, 1991). Anomalies of heat and salt calculated along isopycnal surfaces indicate that the cross-Stream fluxes attributed to ring formation are less than those required to balance property budgets (Bower *et al.*, 1985). Thus other processes make significant contributions to the cross-Stream transfer of properties and biota.

At present, the descriptions of cross-Stream exchange mechanisms are mainly limited to the mesoscale, with the majority of observations from satellite imagery, ship-based surveys, and Langrangian float trajectories. For example, sea surface temperature (SST) imagery and concurrent field sampling has shown that frontal eddies along the edge of the Gulf Stream are the principal mechanism by which Gulf Stream water is transferred onto the shelf south of Cape Hatteras (Lee *et al.*, 1981). These features also influence the local productivity gradients, since the upwelling of nutrient-rich water from the Gulf Stream pycnocline into frontal eddies supports a large fraction of the total annual 'new' productivity of the South Atlantic Bight (SAB; Lee *et al.*, 1991). Similar eddies, and larger features, also likely transfer large volumes of Gulf Stream water into the Slope waters northeast of Cape Hatteras, although there is less information on their potential influence on plankton dynamics (Churchill and Cornillon, 1991).

The trajectories of RAFOS floats describe the exchange process in the main thermocline. Isopycnal floats deployed in the Gulf Stream near Cape Hatteras generally remain in the current until they encounter large meanders between 72 and 70W (Bower and Rossby, 1989). At meander crests the floats cross the Stream toward the cyclonic (northern) edge of the current, and are frequently expelled from the stream at the western (upstream) edge of crests and troughs. Alternatively, floats in the Slope water can cross the front and be re-entrained into the Stream on the downstream edge of crests. In general, float trajectories are consistent with models which predict that water parcels most frequently escape the Gulf Stream at meanders (Bower, 1991; Dutkiewicz *et al.*, 1993), especially when the current is interacting with a ring (Dewar and Flierl, 1985; Nof, 1986).

While it is clear that mesoscale features contribute to the exchange of Gulf Stream water across the front, less is known of the contribution of finescale processes (e.g., Tang *et al.*, 1985). A limited number of studies which have examined the front show it to be a site of active mixing (e.g., Williams, 1981; Lillibridge *et al.*, 1990). We surveyed the surface waters adjacent to the Gulf Stream front between 73 and 71W with an initial intent of examining the finescale structure of a cyclonic eddy. This survey followed a study of shelf water entrained along the edge of the Gulf Stream with an undulating profiler, the Seasoar (Lillibridge *et al.*, 1990). The central objective of this survey was to determine if the eddy-like features east of Cape Hatteras were similar in structure to frontal eddies of the SAB. However, a feature examined with the Seasoar east of Cape Hatteras will be designated as a cyclonic eddy, since its structure was distinct. Following the study of the cyclonic eddy, the opportunity arose for the Seasoar to map a complex region between a warm-core ring and the Gulf Stream. This intensively-stirred region contained filaments of Shelf and Gulf Stream water which were wrapped around the ring, known as streamers, as well as smaller intrusive features. Stirring is here defined as those processes which increase property gradients, as in the formation of streamers, while mixing corresponds to the small-scale processes which diffuse the fields (Garrett, 1983).

An overview (Section 2) describes the evolution of the mesoscale features during the survey and provides a timeline of sampling activity. The structure of the surface layer is described from property sections of temperature, salinity, density and, where available, chlorophyll fluorescence in three Seasoar transects (Section 3a). One transect is presented from the survey of the cyclonic eddy, and two are from the region between the ring and Gulf Stream front. Surface velocity vectors are derived from ship's drift, with a description of the subsurface velocity field from float trajectories and expendable velocity profilers (Section 3b). Indices of mixing activity were computed from the Seasoar data (Section 3c). Finally, the biomass and composition of microplankton communities are described for the Gulf Stream and two streamers (Section 3d). The objective of the plankton sampling was to determine whether or not the netplankton communities in streamers retained the biological characteristics of the source waters. In the Discussion the observations are interpreted in terms of the stirring and mixing processes which mediate the exchange of Gulf Stream water across the front.

2. Overview

a. SST imagery

The development of the cyclonic eddy and the interaction of the ring with the Gulf Stream is described in Lillibridge *et al.* (1990) as four color SST images taken between Oct. 6 (Year Day 279) and Oct. 8 (YD 281), 1985. The major details of these images are reproduced as schematics to describe the evolution of the features examined with the Seasoar (Fig. 1). The subsequent SST imagery collected during
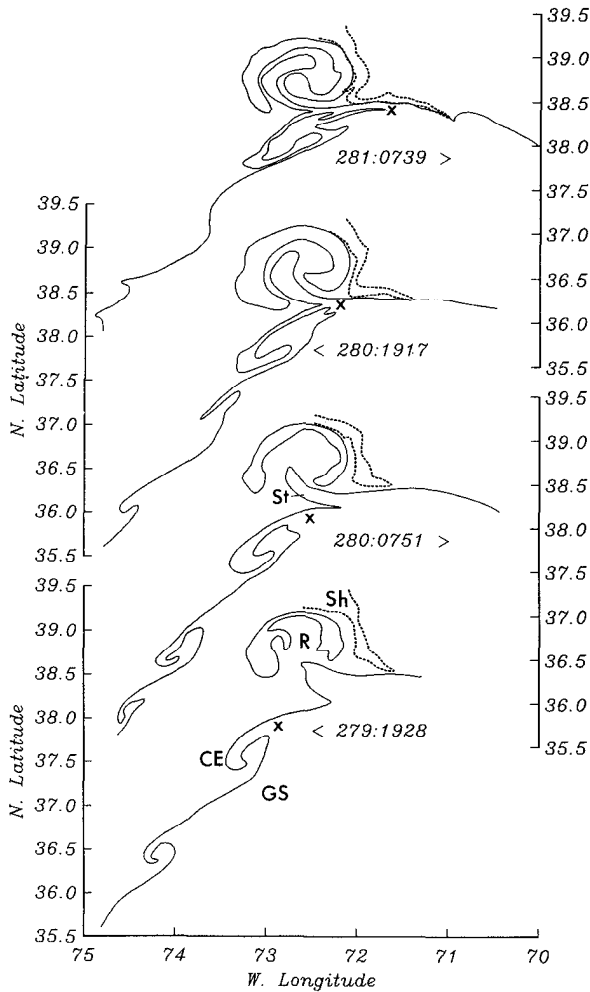
Figure 1. Schematic view of the Gulf Stream front derived from the SST imagery on Year Day 279 to 281 from Lillibridge *et al.* (1990). Time of imagery follows the Year Day; e.g. 279:1928 corresponds to an image on Year Day 279 at 19:28 GMT. The four plots are aligned in longitude and offset with corresponding latitude to the left (YD 279:1928; YD 280:1917) or right (YD 280:0751; YD 281:0739). CE corresponds to the cyclonic eddy, GS is the Gulf Stream, St is a Gulf Stream streamer and x designates its point of attachment to the front. The dashed area (Sh) is a shelf water streamer and R is the warm-core ring.

the survey of the cyclonic eddy and ring is presented in four black-and-white images in Figure 2.

The cyclonic eddy (CE) was first identified on YD 279 as a filament of Gulf Stream water attached to the Stream front near 38.0N, 73.0W (Fig. 1). Two similar filaments were present upstream, at 36N and 37N, but these features dissipated within a day.
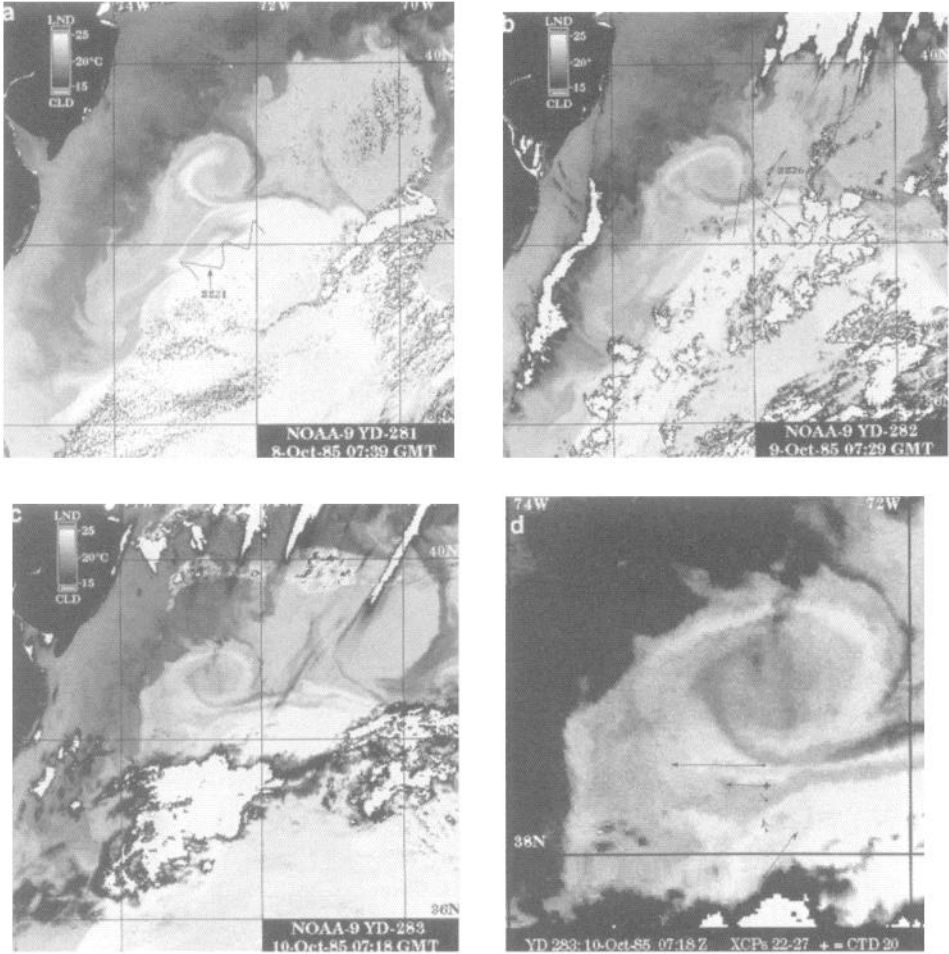
Figure 2. Sea Surface Temperature imagery from the AVHRR sensor onboard NOAA-9 with Year Day and time of image in GMT. SST is accurate to a degree Celsius at a resolution of 0.1°C, with latitude and longitude accurate to ≈ 1 km. Solid lines in (a) and (b) depict the positions of SeaSoar transects underway at the time the images were taken. Image c from YD 283, 07:18 GMT illustrates the elongation of the streamers about the warm-core ring. A portion of this is enlarged in (d) with positions of XCP deployments. Velocity vectors are the mean between 50 and 100 m (arrows). The position of CTD station 20 is plotted (cross), although the station was occupied several hours after the image.

The filament of warm Gulf Stream water which defined the cyclonic eddy doubled in length between YD 279 and 281. The western tip of the cyclonic eddy remained near 73W throughout the three day lifetime of the feature, while the eastern end of the warm filament was advected east with the Gulf Stream at ≈ 0.7 m s⁻¹ ('x' in Fig. 1). The warm filament split to form a streamer (St) which wrapped around a warm-core

ring (R in Fig. 1). This streamer was eventually separated from the original warm filament by a narrow band of cool surface water (Fig. 2b,c). On YD 283 the warm filament of Gulf Stream water, which had originally defined the cyclonic eddy, was stretched parallel to the Gulf Stream front over two degrees of longitude (Fig. 1c).

During the study a cool Shelf water streamer was present on the eastern edge of the ring. On YD 280 the Shelf water streamer extended south from the Shelf/Slope front to the Gulf Stream front (Sh in Fig. 1). Thereafter the Shelf water streamer was entrained about the southern edge of the ring, and within three days it had reached the western edge. In the SE corner of the ring the Shelf water streamer was eventually split into two distinct sections by warmer surface waters (Fig. 2d). A magnified view of the SST image from YD 283 shows that the Shelf water streamer was completely wrapped around the ring, and encircled by the warmer Gulf Stream streamer (Fig. 2d).

b. Sampling Protocol

The finescale structure of the Gulf Stream front was resolved by mapping the property distributions with a Neil Brown Mark III CTD and Q-fluorometer in the Seasoar (Pollard, 1986). The transects extended to a maximum of 160 db, but the fluorescence profiles were limited to a maximum of 100 db due to limitations in logging the data. The survey periods ranged from 14 to 26 hours (Fig. 3) with each transect run at an oblique angle to the Gulf Stream axis (Lillibridge et al., 1990; Anonymous, 1986). Thus in each survey period the features were crossed in successive transects at various angles, so the width of the streamers and intrusive features are less than they appear in the section plots. The orientation of the transects was based on SST information relayed to the ship courtesy of the Remote Sensing Group at the University of Rhode Island. Each survey period was followed by CTD stations, plankton sampling stations, and deployments of an isopycnal float or expendable current profilers (XCP) in the larger features identified from the property sections.

The survey of the cyclonic eddy was begun on YD 281 with six Seasoar transects numbered 20 to 25 (Fig. 3). The orientation of Seasoar transect 21 (SS 21) is shown in Figure 2a. Following the survey of the eddy, the ship was located in the crest of a Gulf Stream meander southeast of the warm-core ring. The warm-core ring was identified in NOAA SST imagery as WCR 63 and had formed in May, 1985 at 40.0N, 62.5W (Anonymous, 1985). This ring was subsequently re-absorbed by the Gulf Stream near Cape Hatteras in December, 1985.

On YD 282 a plankton sampling station was completed in the Gulf Stream with CTD 13 (Fig. 3). Each plankton station consisted of a CTD cast with Niskin bottle samples at discrete depths, followed by a series of pumped samples for microzooplankton biomass and species identification. Following the plankton station in the Gulf Stream, the ship resumed Seasoar transects to the west, repeatedly crossing the
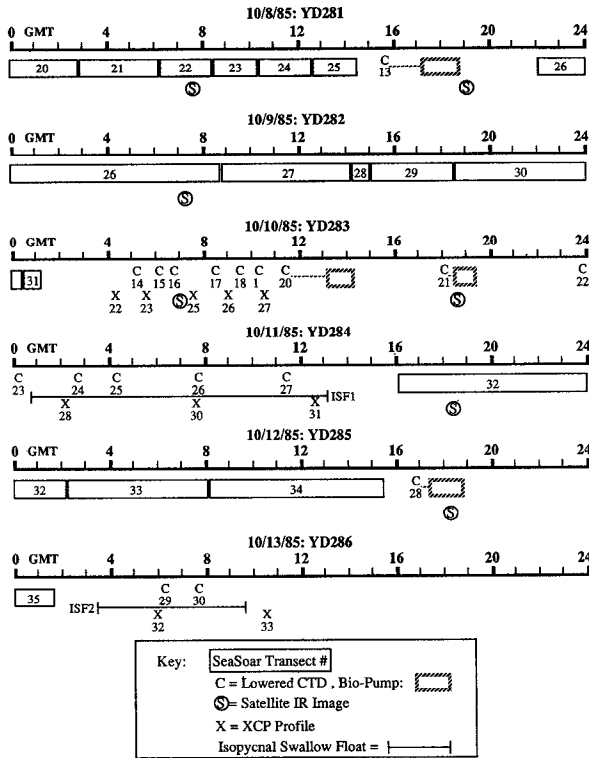
Figure 3. A timeline of sampling activities for YD 281 to YD 286, 1985. The SeaSoar transects are consecutively numbered from 20 to 35 following the sequence described in Lillibridge *et al.* (1990).

region between the warm-core ring and the Gulf Stream front. Two of these Seasoar transects are depicted in an image taken during SS26 (Fig. 2b). After the Seasoar transects were completed, a series of XCP deployments and CTD casts were run north from the Gulf Stream to the ring along 72.75W. This CTD transect was followed by plankton stations at CTD 20 and 21 to characterize the plankton communities of the Gulf Stream and Shelf water streamers, respectively.

On the next day, YD 284, an isopycnal Swallow float was launched in a subsurface intrusive feature north of the Gulf Stream front. This deployment provided a description of the short-term evolution of the intrusive feature from a series of concurrent CTD casts and XCP deployments. After the float was retrieved, three Seasoar transects were run west of the meander crest (SS 32–34, Fig. 3). The property fields from one transect, SS 32, are compared to those from SS 26 in Section 3. A final Seasoar transect was completed on YD 286 with a second deployment of the ISF. These latter observations are not considered here.

c. Methods

All of the available SST imagery from the Advanced Very High Resolution Radiometer (NOAA 9), as well as a description of the Seasoar operation, is provided in a Technical Report (Anonymous, 1986). Briefly, one up/down cycle of the Seasoar required approximately 5 min to complete at a nominal tow speed of 7 knots. This produced two profiles every km. The vertical axis of the property sections from the SeaSoar are expressed as pressure (dbars), while those for the lowered CTD and Niskin bottle casts are as depth (meters). Fluorescence values from the Q-fluorometer are given as relative values with each unit corresponding to 0.1 volt. Relative fluorescence values are plotted, rather than absolute values, since the transects span the depth of the euphotic zone and, in some cases, encompass a solar day. Thus the ratio of fluorescence/unit chlorophyll likely varied during the tows. In general, however, the vertical distributions from the fluorescence plots agree with the vertical pigment profiles from extracted samples taken at individual stations.

The surface velocity field was derived from ship's drift vectors. The vectors were computed as the difference between the ship's heading and course over ground at intervals of 5 min and judged to be accurate to ≈ 5 cm s^{-1} (Anonymous, 1986). The subsurface circulation was observed with two types of Lagrangian drifters. A ship-tracked isopycnal Swallow float was deployed to examine short-term variability in the property fields and velocity in an intrusive feature. The float recorded pressure and temperature at 5 minute intervals with data relayed to the ship by an acoustic link (Rossby *et al.*, 1985). The ship-tracked float operation is limited to periods of days. The RAFOS floats, in contrast, are expendable instruments which provide records of position, temperature and pressure for periods of several weeks (Rossby *et al.*, 1986). The stored data on depth, pressure and position, relative to stationary acoustic beacons, is relayed to shore via System Argos after the float surfaces. Three RAFOS floats were deployed north of the Stream front to examine the exchange between the Slope water and Gulf Stream.

Property distributions from the SeaSoar transects were analyzed after the cruise to derive three indices of mixing processes. Two of the indices are qualitative indicators of mixing, tau (τ) and the conductivity Cox number (C_c), while the third index, the Turner angle (Tu), provides a more quantitative measure of the nature of mixing processes. The variable tau is computed as an orthogonal to σ_θ in the θ/S plane (Veronis, 1972); it serves as a dynamically-passive variable which indicates the tendency for mixing to occur along isopycnal surfaces. If isopleths of τ parallel isopycnal surfaces, then lateral mixing has recently occurred. Conversely, if τ varies along an isopycnal surface then contrasting water types have recently been brought into contact, but there has been insufficient time for complete mixing to occur. The calculation of tau in this report is based on the formulation of Veronis (1972). Jackett and McDougall (1985) derive a revised index to yield a more quantitative indicator of

mixing. Here we rely upon the original formulation as a purely qualitative descriptor of mixing by examining the thermohaline variations along an isopycnal surface.

The conductivity Cox number serves as a nondimensional indicator of microstructure which relies upon the rapid response of the conductivity cell in the CTD, in contrast to the slower response time of the thermistor (Georgi *et al.*, 1983). Local conductivity Cox numbers are similar to the thermal Cox number, and expressed as the ratio of the variance of the conductivity signal normalized to an average over a given depth interval:

$$C_c = \overline{\left(\frac{\partial c'}{\partial z}\right)^2} \left(\overline{\frac{\partial c}{\partial z}}\right)^{-2} \tag{1}$$

where c' represents deviations of the conductivity signal from the mean, and z is depth. The details of computations for the Seasoar data are discussed in Lillibridge *et al.* (1990). Since the nominal tow speed of the Seasoar was 3.5 m s^{-1}, and the sampling rate of the conductivity cell was 31.25 Hz, the along-track resolution of the conductivity signal was estimated to be one measurement every 0.11 m. This resolution is about ten-fold less than that of rapid response thermistors in free-fall vehicles (Oakey and Elliott, 1977), and is comparable to the vertical resolution of a lowered CTD (Georgi *et al.*, 1983). Thus the ability of the towed SeaSoar to resolve microstructure events is nearly an order of magnitude less than that of high-resolution thermistors in microstructure instruments. Nevertheless, the C_c distributions serve as useful measure of 'quiet' and 'active' mixing regions (Georgi and Schmitt, 1983). The C_c were not contoured in the SeaSoar transects since the highest gradients occurred at scales of <1 m.

A third index derived from the CTD records, the Turner angle, yields information on the nature of double diffusive processes. The Turner angle is derived from the local temperature and salinity gradients:

$$Tu = \tan^{-1}\left[(\alpha T_z - \beta S_z)/(\alpha T_z + \beta S_z)\right] \tag{2}$$

where α and β are the thermal and haline expansion coefficients, respectively, and T_z and S_z are the vertical temperature and salinity gradients, respectively (Ruddick, 1983). Thermal and haline expansion coefficients were computed as in Lillibridge (1989). Following the convention of Washburn and Käse (1987), a negative Tu indicates static instability which is likely the result of instrument error. The octant from $135° < Tu < 180°$ indicates conditions unstable to double diffusive layering (temperature destabilizing), and that from $0° < Tu < 45°$ indicates conditions unstable to salt fingering. In both cases an appropriate Tu is a necessary condition for, but not guarantee of, the development of double diffusive mixing processes. A Tu between 45° to 135° corresponds to an interval of the water column stable to diffusive processes. The estimate of Tu was computed from a 10 sec average of T_z and S_z. In a

previous survey of the Gulf Stream front with the Seasoar (Lillibridge *et al.,* 1990), the distribution of mixing processes was interpreted in terms of C_c and Tu at the boundary of entrained Shelf water features known as Ford Water (Ford *et al.,* 1952). Here the indices are used to define regions of mixing in Gulf Stream and Shelf water streamers, and the property fronts of the Gulf Stream and ring.

Plankton samples were collected at 'Bio-Pump' stations (Fig. 3) with CTD casts. Niskin bottles were sampled for pigment biomass and phytoplankton productivity with chlorophyll *a* concentrations and primary productivity rates estimated from at the 100%, 60%, 32%, 17% and 1% isolumes, as described in Lillibridge *et al.* (1990). Bacterial biomass was estimated from Niskin bottle samples by DAPI-stained cell counts with bacterial production rates based on the incorporation of ^{3}H-(methyl)-thymidine (see Børsheim, 1990). The microplankton fraction, composed of organisms > 5 μm, was enumerated from whole-water samples collected from the Niskin bottles and preserved in a refrigerator with 1% glutaraldehyde. Heterotrophic dinoflagellates and ciliates were counted by means of an epifluorescent microscope following staining with DAPI and proflavin. A separate aliquot was counted to enumerate diatoms. Depth-integrated samples were collected from specific intervals with a large-volume pumping system though a 7.5-cm diameter hose to sample the larger, rarer net-microplankton retained in on-board 20 μm plankton nets. The pumped samples primarily contained heterotrophic dinoflagellates, tintinnids, and copepod nauplii. Samples were preserved as above and settled in 10 or 25 ml chambers before examination under the microscope.

3. Results

a. Property sections

i. The Cyclonic eddy. The property fields show the structure of the warm surface filament of the eddy at the northern end of the Seasoar transects. Temperature and salinity sections from SS 21 show the warm filament was well-defined by the 25°C isotherm and 36 psu isohaline. The filament was shoreward of a low-salinity Ford Water feature (salinity < 35.4 psu) which was adjacent to the Gulf Stream property front (Fig. 4a,b). The warm filament of Gulf Stream water had a distinct structure; the 25°C isotherm extended to the base of the filament, at 45 dbars, while in the Gulf Stream it deepened to ≈ 85 dbars (Fig. 4a). The most prominent expression of the cyclonic eddy, however, was in the salinity field. The filament was clearly defined in all transects as a series of concentric isohalines inclined towards the Gulf Stream front. In SS 21 the 36 psu isohaline deepened to > 120 dbars, extending below the fresher Ford Water feature. The Ford Water had been previously mapped as a continuous band of Shelf water which extended north from 35.50N, 74.30W along the Gulf Stream front (see Lillibridge *et al.,* 1990). Strong horizontal gradients in salinity and temperature were consistently found along the entire length of the Gulf Stream
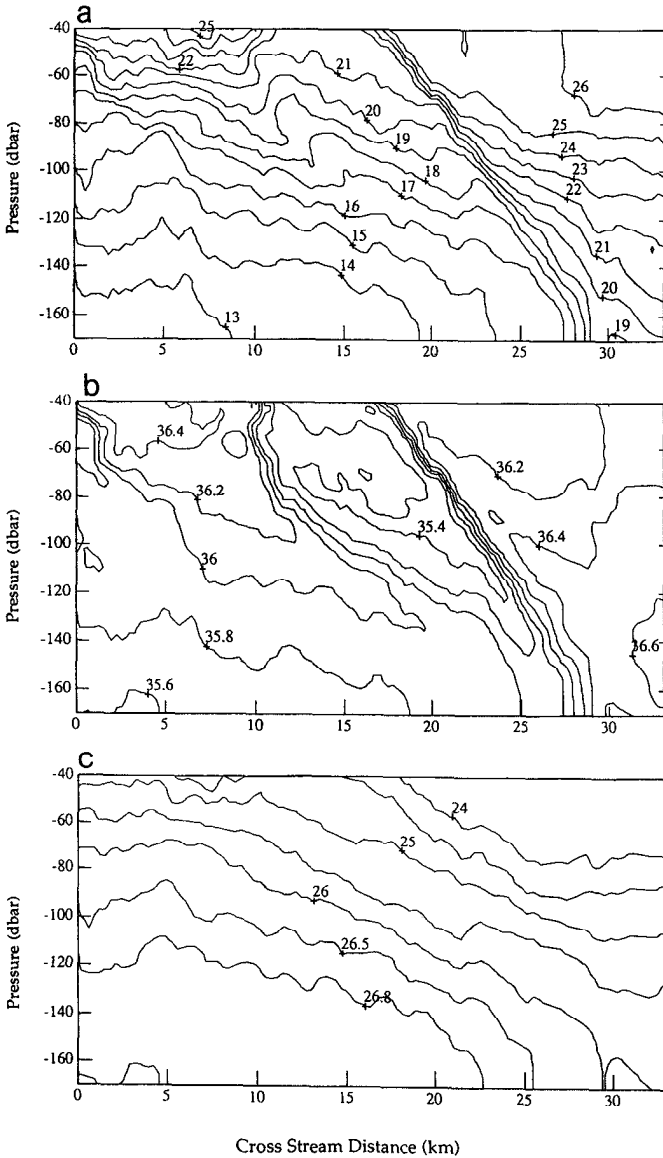
Figure 4. Property sections of temperature in °C (a), salinity as psu (b), and density as σ_θ (c) from SeaSoar transect 21. The orientation of the transect across the western end of the cyclonic eddy is shown in Figure 2a.

front. In SS 21 the north wall of the Gulf Stream, defined by 15°C at 200 dbars, was ≈ 25 km SE of the origin of the transect.

The isopycnal surfaces shoaled from the Gulf Stream front to the center of the cyclonic eddy at a slope approximately half that of the isotherms and isohalines. The
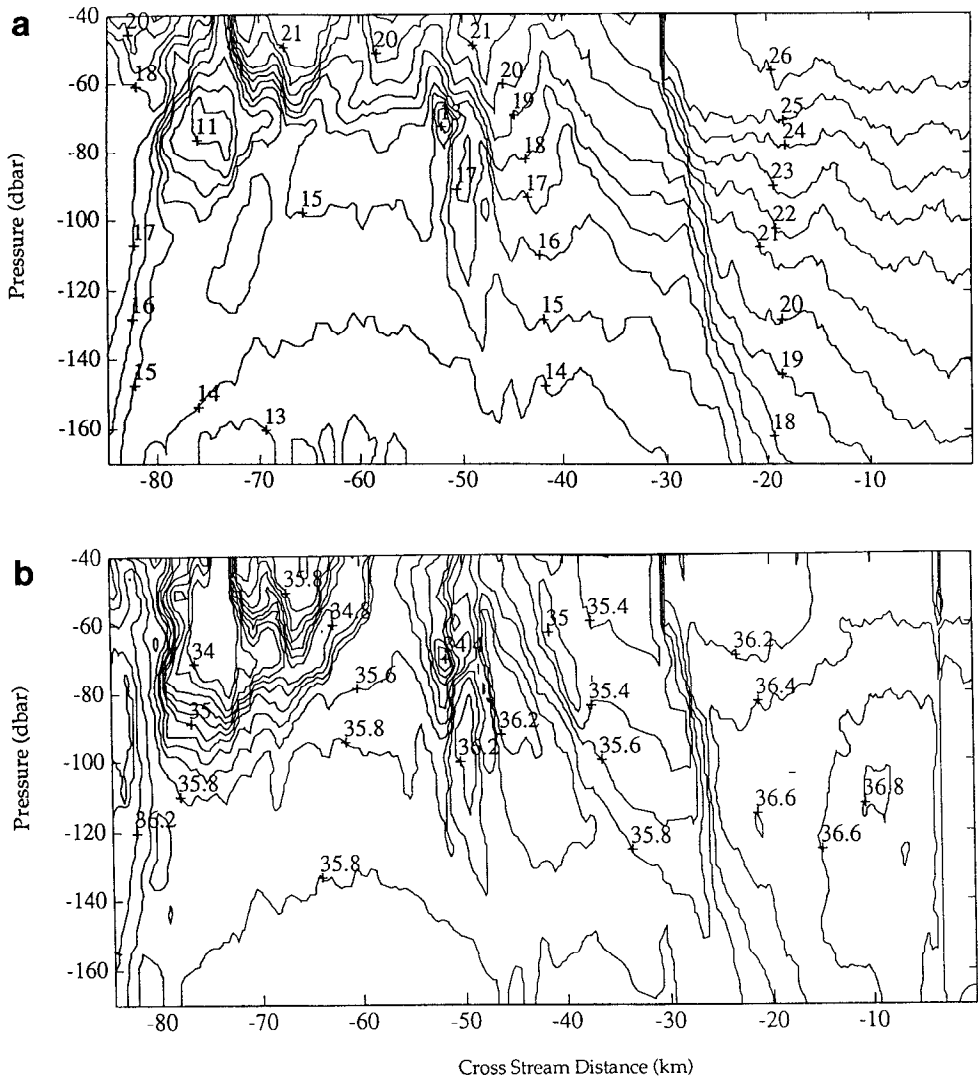
Figure 5. Same as Figure 4, but for SeaSoar transect 26. The orientation of SS 26 is shown in Figure 2b. Panel (d) is a section of relative chlorophyll fluorescence (volts × 10). The vertical lines in salinity and density near −3 km are due to biofouling of the conductivity sensor.

T/S isopleths of the warm filament and the Ford Water feature were inclined to the density surfaces. These patterns were consistent with observations of intrusive features surveyed upstream, near Cape Hatteras (Lillibridge *et al.,* 1990). In general, there was less finescale variability evident in the isopycnals than in either the isotherms or isohalines (Fig. 4c). The small-scale variations in the depth of the isopycnals was about 10 dbars, likely due to internal waves.
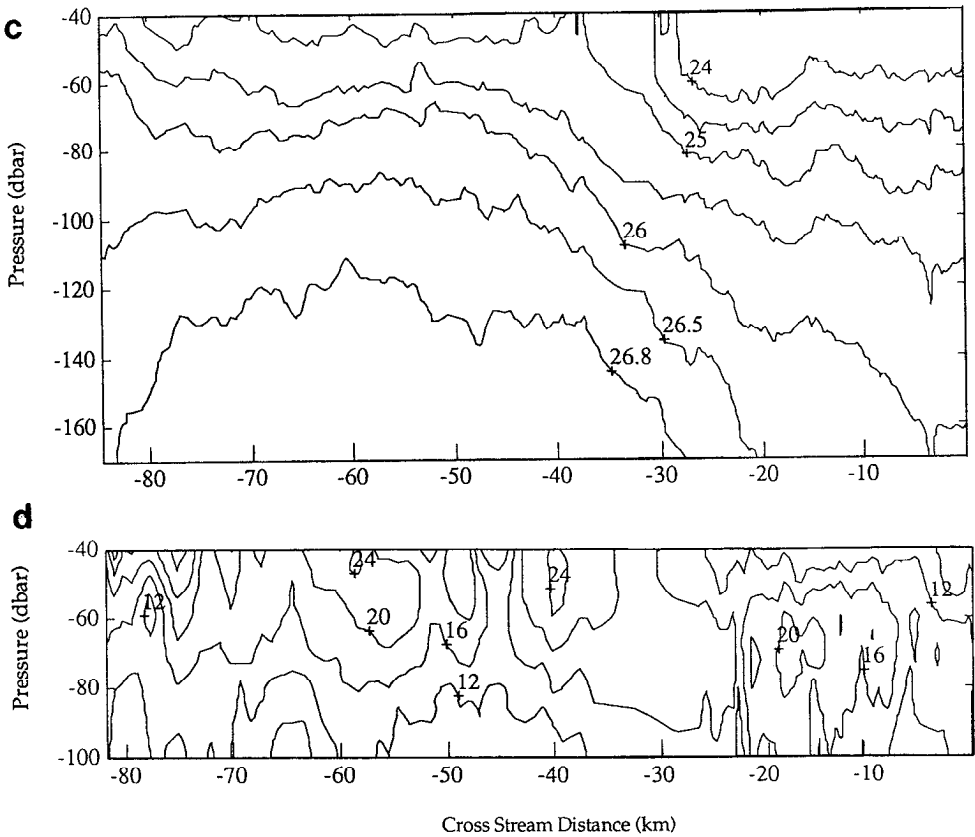
c

d

Cross Stream Distance (km)

Figure 5. (Continued)

ii. Gulf Stream / Ring Interaction. The interaction between the warm-core ring and Gulf Stream produced a complex pattern of surface filaments and streamers, as well as subsurface intrusive features. The survey of these features began with Seasoar transect 26 which coincided with a SST image (Fig. 2b). The typical features of the Seasoar sections are shown by the property fields from SS 26 in Figure 5 (T, S, σ_θ, chlorophyll fluorescence). Since the transect was run from south-to-north, the distance along the section is plotted as negative km. The data at −3 km, and between −28 and −37 km, was lost due to fouling of the CTD sensors; the property isopleths between −28 and −37 km have been interpolated.

The largest features in the property sections coincide with the thermal fronts seen in the SST imagery. The conspicuous property front of the Gulf Stream, for example, coincided with the location of the surface front in the SST image (cf. Figs. 2b, 5a). As in all other sections, the Seasoar transect revealed a subsurface, low-salinity Ford Water feature adjacent to the Gulf Stream front (Fig. 5b). In contrast to the Ford Water feature near the cyclonic eddy, however, the core of the low-salinity water in

SS 26 (35 psu) was displaced several km shoreward of the Gulf Stream property front. Additionally, the minimum salinity in the Ford Water feature in SS 26 was ≈ 0.4 psu fresher than that in SS 21. This downstream fluctuation in the strength of the salinity of Ford Water may reflect variability in the source of the entrained Shelf waters (see Lillibridge *et al.,* 1990).

There were several narrow low- and high-salinity intrusive features between −30 and −60 km (Fig. 5b). These finescale intrusions had widths of < 5 km, and were 20 to 60 meters thick. Since the orientation of the transect was at an oblique angle to the fronts, the width of the finescale intrusions was likely on the order of a km. One intrusive feature had a core salinity of 36.2 psu which implies an origin from the Gulf Stream (−50 km, 80 to 120 dbars in Fig. 5b). This high-salinity feature was bordered by a cooler, low-salinity intrusion with a core of 34.4 psu, 13°C water centered at −52 km and 70 dbars. The signature of this feature implies a Shelf water origin. These two features are examined in terms of mixing indices in Section 3c.

At the northern end of the transect the warm-core ring was clearly evident as a thermostad of 17°C water with a salinity > 36 psu (Fig. 5a,b). A large volume of low-salinity water adjacent to the ring front, between −70 and −75 km, corresponds to the base of the Shelf water streamer seen in the SST imagery (cf. Figs. 2b, 5b). The minimum salinity in the Shelf water streamer was 34 psu at a temperature of 11°C. The core of the streamer was not uniform, with variability in the salinity and temperature sections reflecting a complex structure. For example, a narrow band of low-salinity water (34.6 psu; 15°C) shoaled from center of the Shelf water streamer to the south. Although this band of low-salinity water was within 15 km of the low-salinity, intrusive feature found at −50 km, each had distinct T/S characteristics.

As in the previous transects, the isopycnals shoaled across the Gulf Stream front with a slope approximately half that seen in the isotherms and isohalines (Fig. 5c). The denser isopycnals ($\sigma_\theta > 26.0$) domed slightly between the Gulf Stream front and the edge of the warm-core ring. At the edge of the ring the isopycnals of $\sigma_\theta > 26.5$ deepened while the shallower density surfaces ($\sigma_\theta < 26.0$) shoaled. The isopycnals did not exhibit the small-scale variability seen in the temperature and salinity fields. The depth of the isopycnals varied by about 10 m over horizontal distances of a few km, similar to the variations seen in SS 21. The fluorescence distribution in SS 26 also lacked the variability seen in temperature and salinity fields (Fig. 5d), although the vertical extent of the section was limited to 40 and 60 dbars. The highest relative fluorescence values (> 20) were observed in the vicinity of the Gulf Stream front, and in a subsurface maximum in the Slope water above 60 dbars. A minimum in fluorescence (< 12) coincided with the base of the Shelf water streamer at −80 km (Fig. 5d).

The property fields were mapped southwest of the ring on YD 284. The first transect in this series, SS 32, extended south along 73W (Fig. 6). The Seasoar was

deployed in the ring, as indicated by the thermostad of warm, salty water at the origin of the transect (Fig. 6 a,b). South of the ring there were several cool, relatively fresh intrusive features which coincided with the location of the Shelf water streamer in the SST imagery (Fig. 2d). These intrusive features were characterized by a minimum salinity of 34.6 psu and temperature of 13°C. The salinity values are ≈1 psu higher, and the temperature 2°C warmer, than that observed in the core of the Shelf water streamer surveyed two days previously in SS 26. The property fields suggest, therefore, that the base of Shelf water streamer had evolved into intrusive features as it was advected about the southern perimeter of the ring.

South of the low-salinity intrusive features there was a larger filament of relatively warm, salty water between 20 and 30 km which extended from the surface to 80 dbars (Fig. 6 a,b). This feature corresponded to the position of the streamer of Gulf Stream water in SST imagery. The salinity of the filament (36.2–36.4 psu) confirms an origin in the Gulf Stream. While the core of the warm-core ring also was composed of relatively salty water, at 36.4 psu, the corresponding temperature in the ring was 17°–18°C, several degrees cooler than that of the streamer (25°C).

South of the streamer of Gulf Stream water there were several narrow warm/salty and cool/fresh intrusive features (Fig. 6a,b). As an example, a cool intrusive feature bordered the Gulf Stream streamer at 30 km and a high-salinity intrusion was centered near 50 km, at 30 dbars. As in all Seasoar transects, a low-salinity Ford water feature was adjacent to the Gulf Stream property front in SS 32. The minimum salinity of the Ford Water was 34 psu, lower than that observed in either SS 21, south of the cyclonic eddy, or in SS 26. This along-stream gradient in the salinity of the Ford Water supports the hypothesis that there is considerable variability in the strength of the source waters (Lillibridge *et al.*, 1990). The section plots from the Seasoar transects therefore show that larger streamers were frequently bordered by smaller intrusive features of contrasting water types, and the structure of the streamers appeared to vary over periods of a few days.

In general the cross-stream distribution of the isopycnal surfaces in SS 32 was similar to that observed in SS 26. The upper pycnocline domed between the Gulf Stream front and the ring with small-scale variability in the depth of the isopycnals on the order of 10 meters. However, there were some differences in the density sections between the two transects. In SS 32 the density surfaces of 25.0–26.5 σ_θ were ≈10 to 15 dbars shallower than in SS 26. Furthermore, the high-salinity, finescale intrusions found near the surface in SS 32 correspond to distinct minima in the density field. In SS 26, in contrast, there was little variability in the isopycnal section associated with intrusive features.

The spatial pattern of chlorophyll *a* fluorescence in SS 32 revealed a subsurface maximum shoreward of the Gulf Stream property front (Fig. 6d). The highest fluorescence values (>20) were generally found in the upper pycnocline between
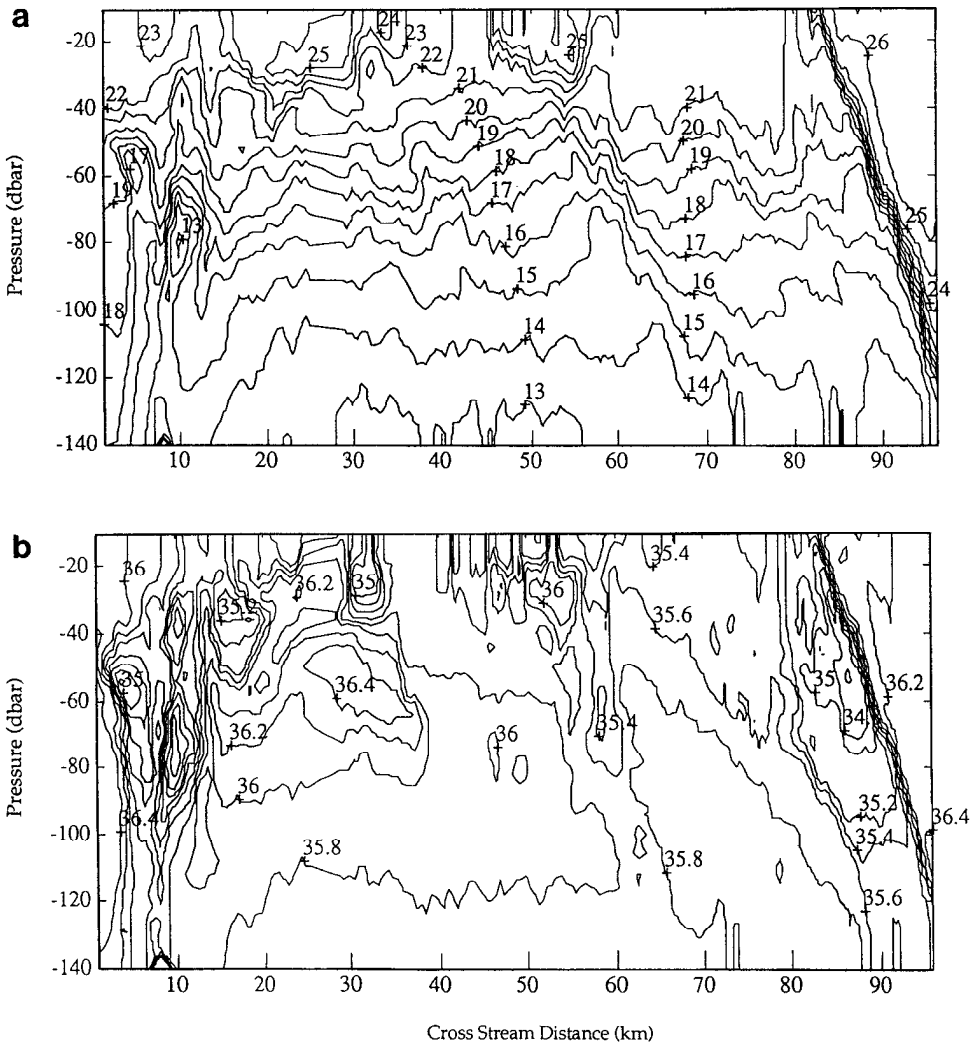
Figure 6. Same as Figure 5, but for SeaSoar transect 32 southwest of the ring.

density surfaces of $\sigma_\theta = 25.5 - 25.0$. As in SS 26 there was less structure evident in the fluorescence field than in the temperature or salinity fields, although a localized maximum in fluorescence coincided with the subsurface Ford Water filament near the Gulf Stream front. Another localized maximum in fluorescence was found at 55 km centered between the shoreward edge of the Ford Water and an adjacent high-salinity intrusive feature. Additionally, relatively high fluorescence values occurred at the southern edge of the ring. This region of low fluorescence value did not, however, correspond to a specific hydrographic feature, since the fluorescence
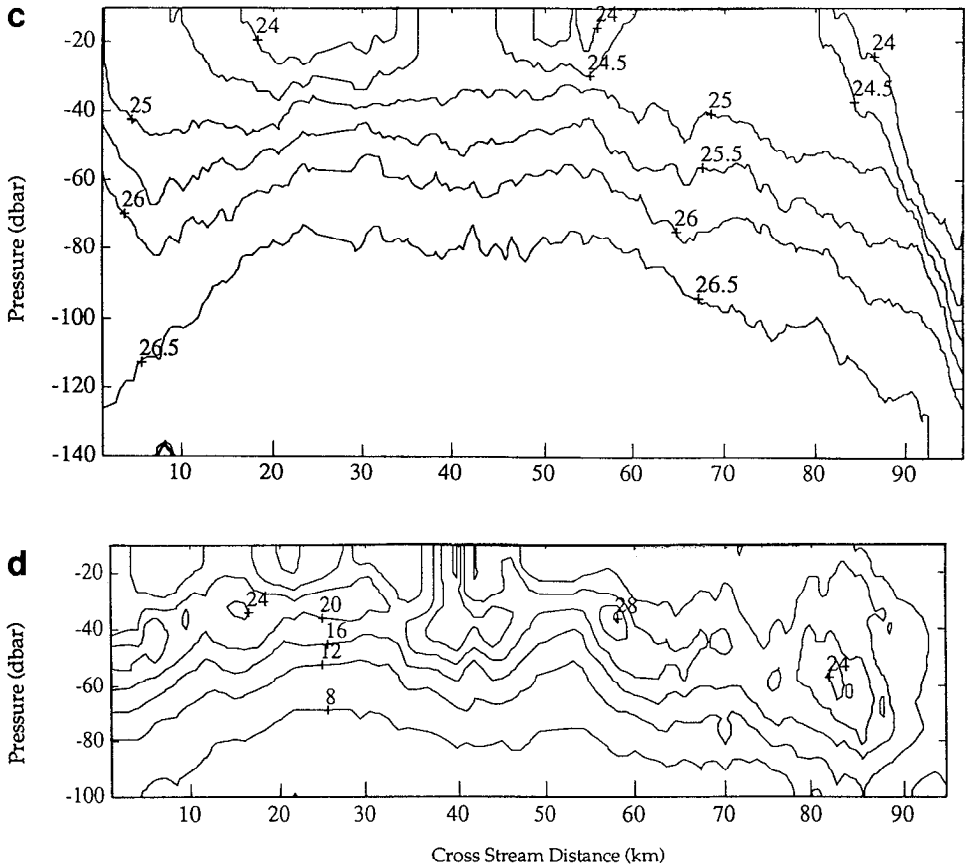
Figure 6. (Continued)

maximum spanned from the edge of the ring to the low-salinity intrusive features (Fig. 6d).

b. Velocity fields

Surface velocity vectors were mapped from the survey of the cyclonic eddy in transects SS 20–25, and from the survey between the ring and Gulf Stream front in SS 26–30 (Fig. 7). Although the surface vectors are not synoptic, they provide a gross description of the surface velocity field shoreward of the Stream front over a period of 48 hours. In the center of the cyclonic eddy the surface velocity was relatively low with maximum speeds < 1.0 m s^{-1} (Fig. 7). The direction of surface vectors indicates cyclonic circulation about the western end of the eddy. This pattern is consistent with the seaward slope of the high-salinity core of the warm filament, as well as the cyclonic motion implied in the SST image. Surface velocities rapidly increased to > 1.5 m s^{-1} as the ship crossed the Gulf Stream front in SS 20 and 21.
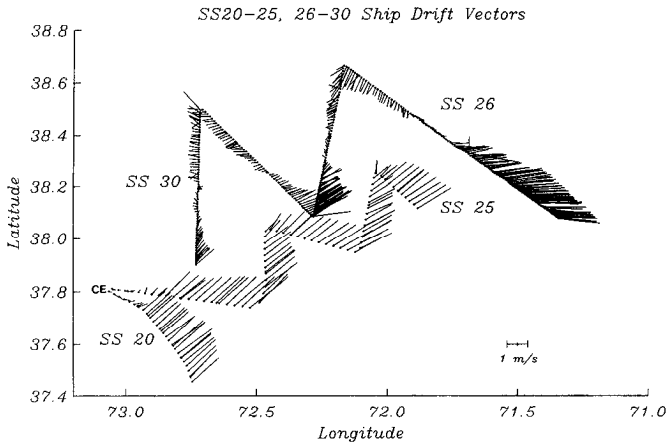
Figure 7. Surface velocity vectors calculated from ship's drift measurements. Vectors from SS 20 to 25 correspond to the survey of the cyclonic eddy on YD 281, with the interior of the eddy designated as CE. Transects SS 26 to 30 depict the surface velocity field from Seasoar survey on YD 282 between the Gulf Stream and warm-core ring.

Surface velocity vectors from SS 26–30 also show a strong gradient at the Gulf Stream front and, at the northern end of transects, the anticyclonic circulation about the perimeter of the ring. The downstream velocity (**u**) was plotted as a function of distance along each transect to derive an estimate of horizontal shear. Shear is expressed as a ratio of f, the Coriolis parameter (Fig. 8). Maximum surface velocities at the edge of the ring were -1 m s^{-1}, to the west, while in the Gulf Stream the maximum surface velocities were eastward at $\approx +1.5$ m s^{-1}. The strong gradient across the Gulf Stream front gave horizontal shear on the order of f. The surface velocity vectors from the ship's drift observations in SS 30 are compared with subsurface vectors derived from XCPs launched 4 to 10 hours later in Figure 9. The fair agreement between the two measurements is interpreted as evidence that north of the Stream front the flow in the mixed layer was consistently westward (Fig. 9). The subsurface flow from XCPs 24 to 30 shows a westward component at ≤ 1 m s^{-1} between 50–100 m (Fig. 9). This subsurface pattern in velocity corresponds to the westward flow evident at the surface. In some XCP records there was vertical shear evident between the surface and 50 m.

A narrow reversal in the surface velocity along SS 30 was found at 38.2N (arrow in Fig. 9). This eastward flow was several km north of the Gulf Stream front and coincided with a narrow band of cool water. This cool band separated the Gulf Stream streamer (north) from the warm filament which previously defined the cyclonic eddy (south). While the SST imagery shows the cool band of Slope water extending to the east, there were no reversals observed in the ship's drift velocity records in the previous transects, SS 26 to 28. This cool filament may have been
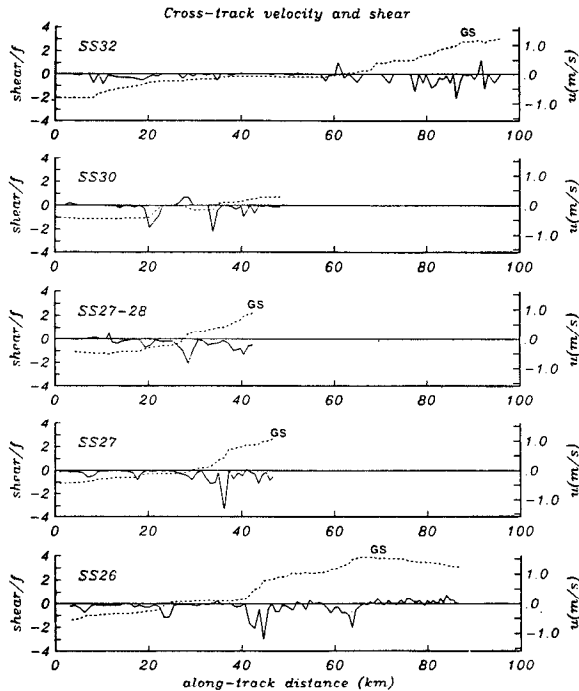
Figure 8. Cross-track velocity (**u**, dashed line) and the ratio of horizontal shear/f (solid line) from ship's drift observations on SeaSoar transects 26 to 32. All transects are aligned at a common origin with their southern end at 100 km. GS = Gulf Stream.

generated by the upwelling of Slope water as the warm surface filament of Gulf Stream water split to form the streamer.

A ship-tracked isopycnal Swallow float (ISF) was launched north of the Gulf Stream front to observe the short-term evolution of a subsurface intrusive feature. The float was ballasted for the isopycnal surface of $\sigma_\theta = 26.4$ and launched at 38.25N, 72.73W on YD284. The launch point was near the mid-point of transect SS 30 from YD 283. The property sections from SS 30 were used to determine the density field in this region. A CTD cast (CTD 23) immediately following the launch of the float indicated the ISF equilibrated at 80 dbars near the intended density surface. A T/S time series constructed from successive CTD casts while following the float shows the instrument tracked the $\sigma_\theta = 26.4$ surface to within 0.1 σ_θ (Fig. 10). Temperature records from the float varied from 16° to 17°C, with corresponding salinity values from the CTD casts ranging from 35.9 to 36.1 psu. Thus the float followed a subsurface intrusive feature which had originated from the Gulf Stream.

During the 12 hour deployment the float drifted WSW at 51 cm s^{-1}, parallel to the surface velocity vectors derived from ship's drift (not shown). The float gradually sank at an average rate of ≈ 0.2 cm s^{-1} to a final depth of 87 dbars. Short-term
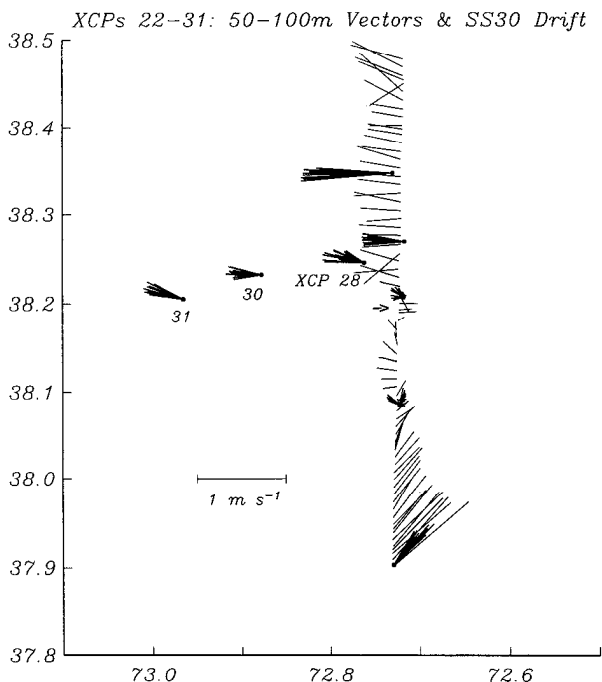
Figure 9. Velocity vectors from ship's drift observations in transect SS30. The reversal in surface current at 38.2N is noted by the arrow. Subsurface velocity vectors for the depth interval of 50 to 100 m are presented in 5 m bin averages from XCPs 22 to 31. XCPs 28, 30 and 31 were deployed while following the isopycnal Swallow float.

variations on the order of 10 m were observed in the depth of the float (Fig. 10). This depth interval was similar to the variability observed in the density surfaces within the Seasoar transects, and is potentially attributed to internal waves. The time series of properties from the CTD casts show the subsurface structure of other intrusive features relative to the float. For example, at launch the CTD identified a Slope water intrusive feature between 50–60 dbars (Fig. 10). When the float was recovered 12 hours later at CTD 27 the T/S properties suggest Gulf Stream water was present between 50–60 dbars.

The complex structure of the surface layer evident in the CTD section (Fig. 10) is consistent with the property sections from Seasoar transect 32, which began 3 h after the float was recovered. Transect SS 32 ran north-to-south, and was oriented nearly perpendicular to the float trajectory. The property sections therefore provide a view of the hydrographic structure of the mixed layer tangential to the flow field. The CTD section (Fig. 10) suggests the isopycnal float remained within a warm, salty intrusive feature which corresponds to a region with similar hydrographic characteristics at 20 to 30 km on SS 32 (Fig. 6). The float therefore appeared to be ≈ 10 km south of the Shelf water intrusive features adjacent to the ring.
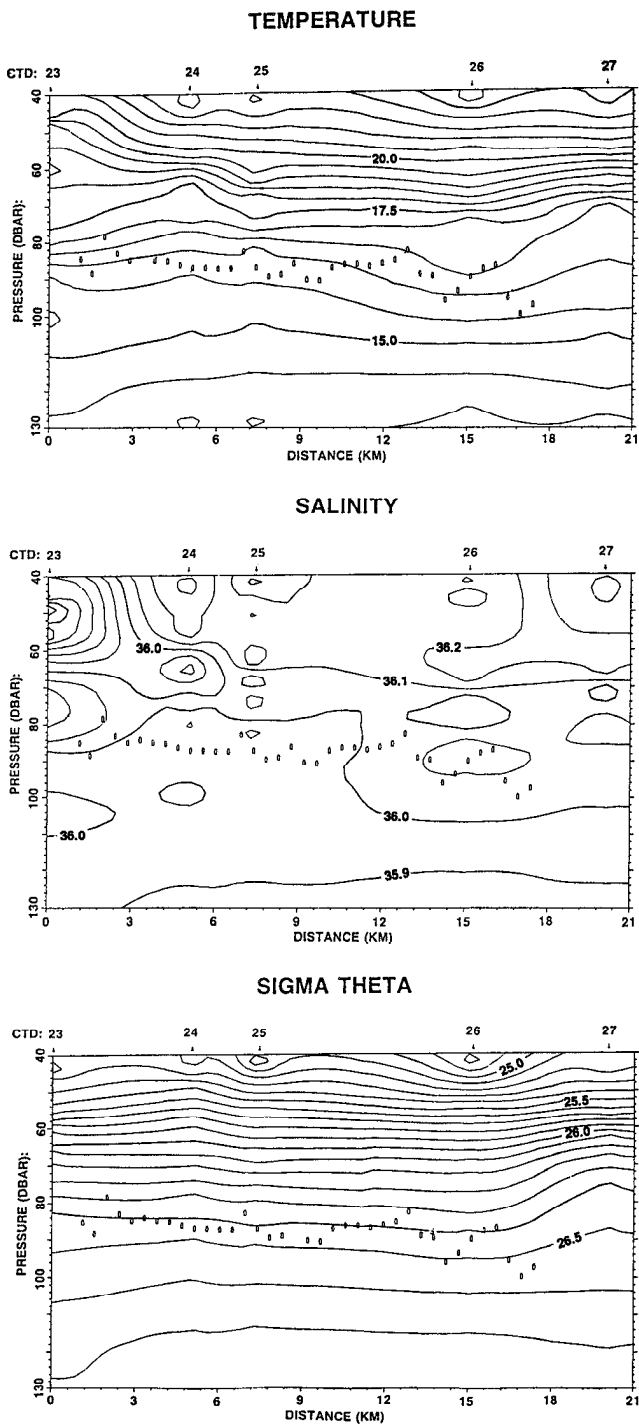
TEMPERATURE

SALINITY

SIGMA THETA

Figure 10. Temperature, salinity, and density (σ_θ) sections from consecutive CTD casts (23–27) during the deployment of the isopycnal Swallow float. The depth of the float is shown by the line figures near the 26.0 σ_θ surface.
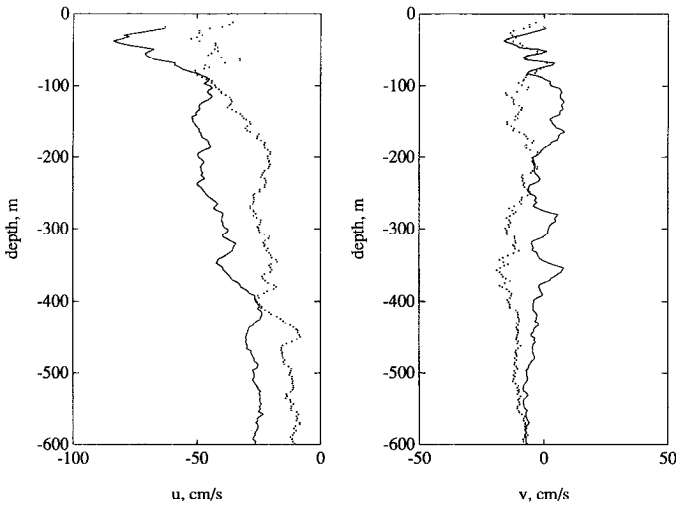
Figure 11. Velocity components as u and v from XCP 28 (solid line) and 31 (dashed line). Probe 31 was launched half an inertial period after probe 28. Both XCPs were deployed while following the isopycnal Swallow float, with the velocities corrected to true north and referenced to the synoptic velocity of the float.

As the ship tracked the float, three XCPs were launched at intervals of one-quarter the inertial frequency, 4.9 hours. The relative velocity profiles from the XCPs were corrected by first rotating the axes to true north, and then referencing the profile velocity at 80 dbars to the synoptic velocity of the ISF. The velocity profiles reveal that the flow was to the west at depths <600 m (Fig. 11). Large vertical shear occurred between 50 and 100 m, on the order of 4×10^{-4} s^{-1}, with the maximum shear in the E-W component. The velocity at the near-inertial period was calculated from XCP 28 and 31 which were separated by half an inertial period. Values for u and v at the near-inertial period were rather high, estimated to be on the order of 10 cm s^{-1}.

A longer-term, Lagrangian view of circulation in the deeper Slope waters is described by the trajectories of three isopycnal RAFOS floats deployed between the ring and the Gulf Stream front. All three floats were ballasted for the 27.0 σ_θ surface and surfaced after 45 days. Two of the trajectories suggest cyclonic circulation at depth (Fig. 12). Float 043, for example, remained at 150 dbar for two weeks. The float was entrained by the Gulf Stream and then subducted to >600 dbars (Bower *et al.*, 1986). A second float, 050, initially reached equilibrium at ≈ 180 dbar. Almost two weeks later the float was entrained by the Gulf Stream and subsequently deepened to 600 dbar as it traversed a meander crest and trough. The third float, 061, remained in the Slope water throughout the 45 day mission. Temperature and pressure records from this float suggest that it maintained an equilibrium on the
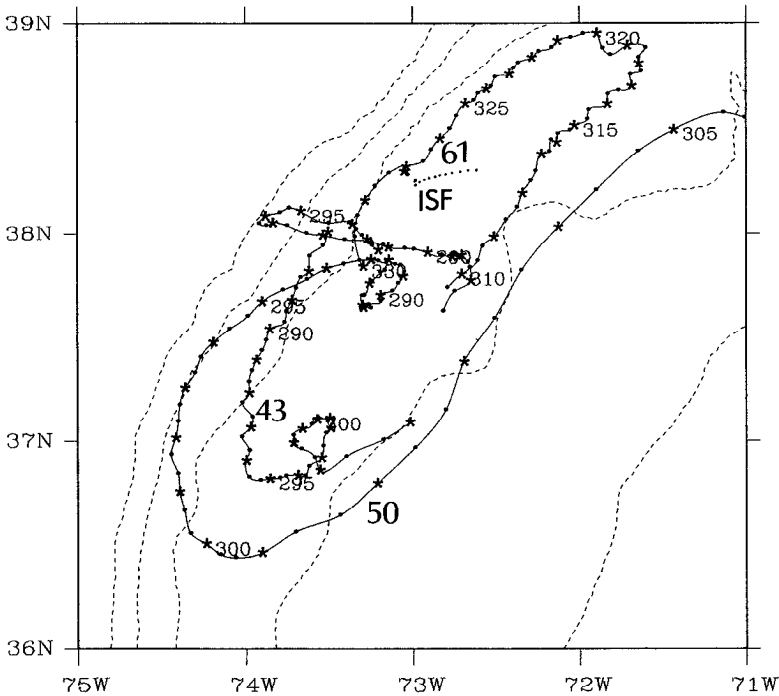
Figure 12. Trajectories of RAFOS floats 043, 050, and 061, and the trajectory of the isopycnal Swallow float (ISF).

27.0 σ_θ surface as temperature varied by 0.5°C, and depth by only 50 meters. The instrument initially drifted WNW, then underwent an anticyclonic turn to the NE and SW (Fig. 12). In summary, the RAFOS floats suggest that water parcels are readily-exchanged between the Slope water and Gulf Stream on time scales of weeks (Bower and Rossby, 1989).

c. Small-scale mixing processes

The three indices of mixing activity derived from Seasoar transects SS 26 and SS 32 suggest that small-scale processes were concentrated at the property fronts. Since the patterns were similar in both transects, only the indices from SS26 are shown. The parameter τ was contoured as a function of pressure, rather than density, since the isopycnals were essentially horizontal between the ring and Gulf Stream front (Fig. 5c). As expected, the highest values of τ correspond to the warm, salty waters of the Gulf Stream and warm-core ring, and lower τ values coincide with cooler, fresher Shelf waters (Fig. 13). The minimum values of $\tau < 4.5$ were located in the Shelf water filament adjacent to the ring. A narrow minimum in the τ field occurred between -40 and -50 km which corresponds to a Shelf water intrusive feature positioned between two Gulf Stream intrusive features (see Fig. 5). All three of the intrusive features had
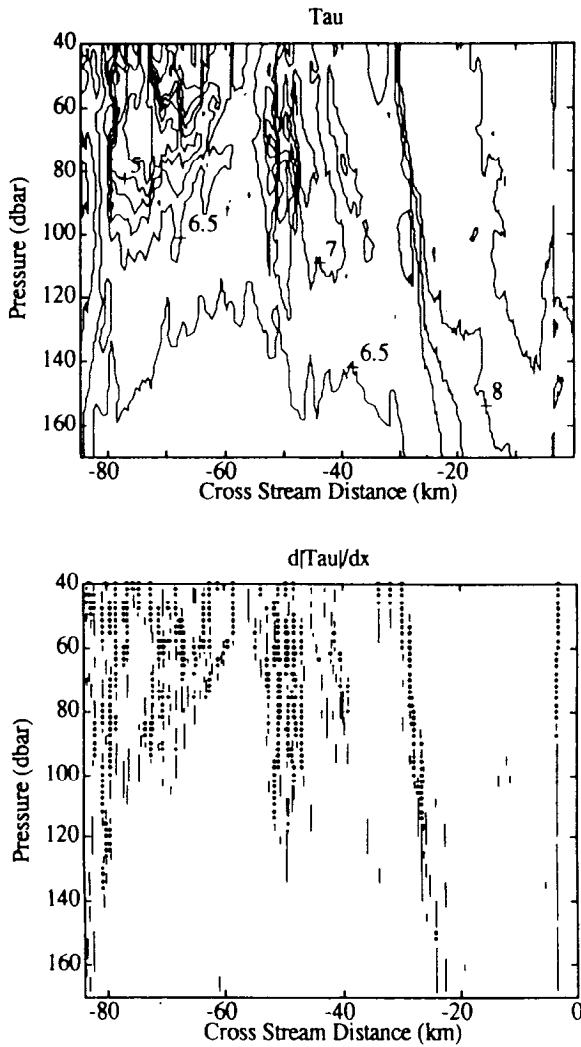
Tau

Cross Stream Distance (km)

d|Tau|/dx

Cross Stream Distance (km)

Figure 13. Section plots from SS 26 of tau (Tau), Turner angle (Tu), the horizontal gradient in tau, $|d(\text{tau})/dx|$ as km^{-1}, and conductivity Cox number (C_c). The Turner angle is depicted for low values ($0 < Tu < 20$, dots) corresponding to the salt fingering case, and high values ($135 < Tu < 180$, vertical line) for diffusive layering. The CTD conductivity sensor was fouled between -28 and -37 km, and also at -3 km. The conductivity Cox number is shown for two ranges ($20 < C_c < 40$, vertical line) and > 40 (dots). For $|d(\text{tau})/dx|$ the vertical lines correspond to $0.2 < |d(\text{tau})/dx| < 0.4$ and dots for $|d(\text{tau})/dx| > 0.4$.

lateral scales of < 2 km and vertical dimensions of 20 to 40 m. The horizontal gradient in τ, $|d\tau/dx|$, was calculated where σ_θ was relatively constant with depth to provide an indication of the relative strength of property gradients along isopycnals. It is clear that the highest horizontal gradients in τ coincide with the strongest
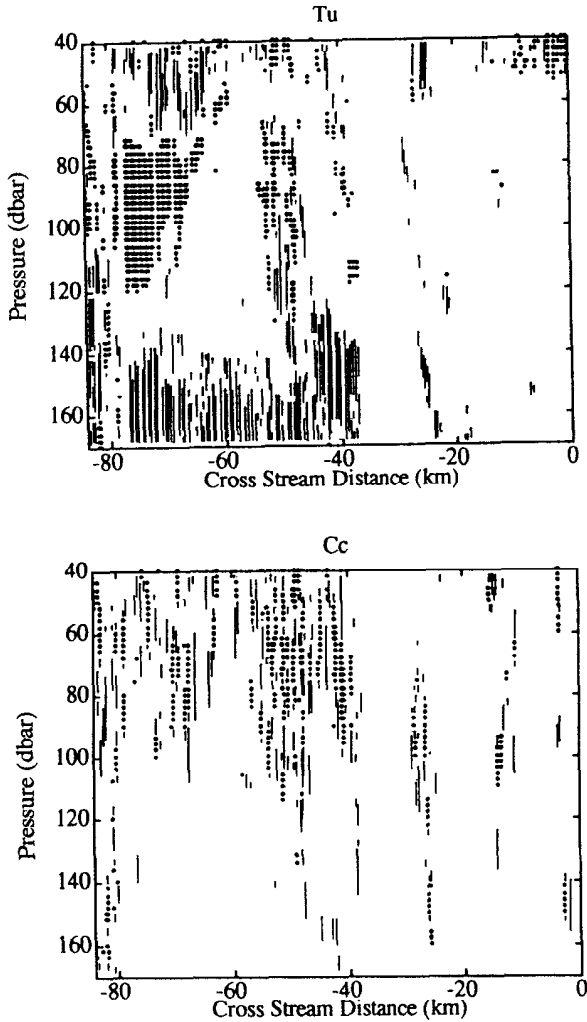
Figure 13. (Continued)

property fronts, particularly at the edge of the Gulf Stream and warm-core ring, as well as the periphery of streamers and intrusive features (Fig. 13).

The conductivity Cox numbers give a qualitative indication of the occurrence of mixing processes at vertical scales on the order of tens of cm (Georgi and Schmitt, 1983). In transect SS 26 the highest C_c were found in the mixed layer at $\sigma_\theta < 26.5$. Below 120 dbars the highest C_c were evident only in the property fronts of the Gulf Stream and warm-core ring (Fig. 13). In general, the highest C_c coincided with the largest horizontal gradient in τ at the property fronts. The strong correspondence between C_c and the τ gradient suggests that interleaving and double-diffusive
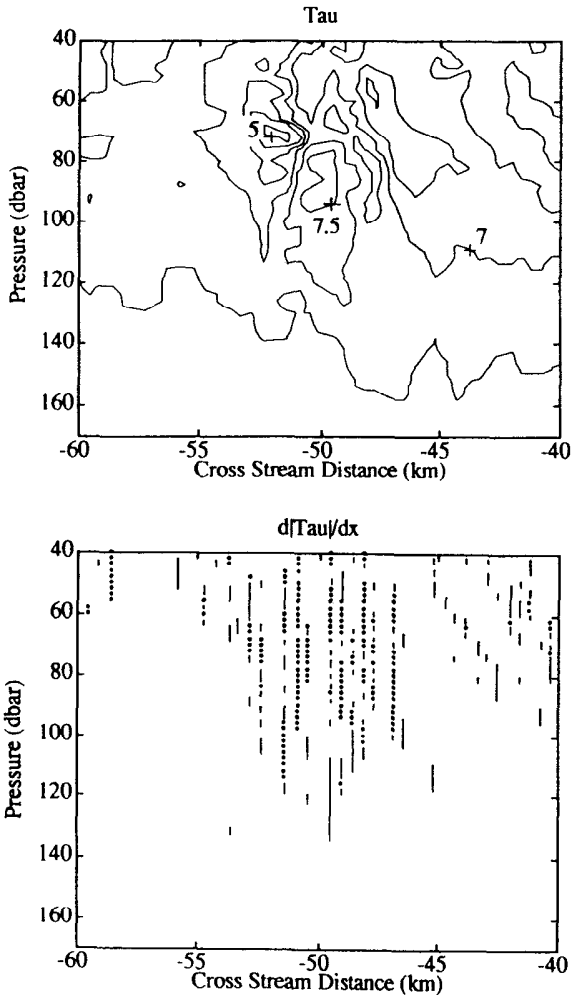
Figure 14. An expanded view of Figure 13 for the region between −60 and −40 km.

processes occurred at the fronts. Individual temperature and salinity traces from the Seasoar transects showed numerous inversions, indicating strong interleaving, at the largest fronts and at the edge of intrusive features.

The distribution of Turner angles from SS 26 suggests the nature of double diffusive processes. Relatively low Tu values occurred where warm, high-salinity waters overlie cooler, fresher waters, where salt fingering would be expected (Fig. 13). Low Tu values were found near the upper boundary of the Shelf water streamer between −65 and −80 km above 60 dbars. Where cooler, fresh waters overlie warmer, saltier waters relatively high Tu values suggest conditions were favorable for diffusive layering. This was observed at the base of the Shelf water filament, below
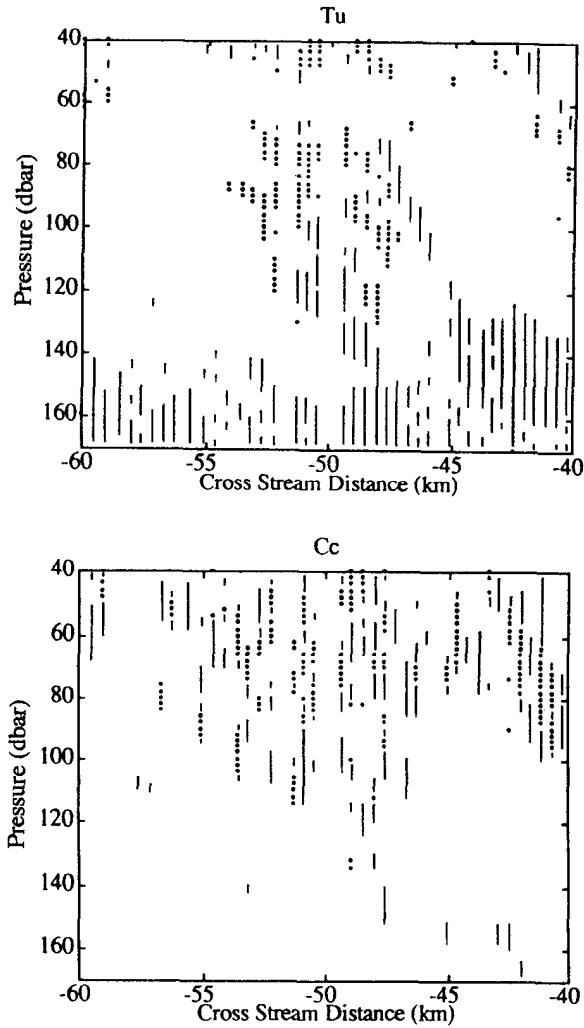
Figure 14. (Continued)

80 dbars (Fig. 13). The extensive region of low *Tu* values below 140 dbars is typical for North Atlantic waters below the pycnocline.

An expanded view of mixing indices is presented for the Shelf water and Gulf Stream intrusive features at −40 to −60 km (Fig. 14). A local minimum in τ corresponds to the shelf water feature (τ = 5.5) at −52 km, while a maximum in τ (> 7.5) coincides with a high-salinity Gulf Stream intrusive feature at −50 km (Fig. 14). The surface velocity vectors indicated relatively weak advection in this region, with isopycnals shoaling by ≈ 5 dbars at the boundaries of two intrusive features. Although the core of the finescale features were relatively homogenous, with small
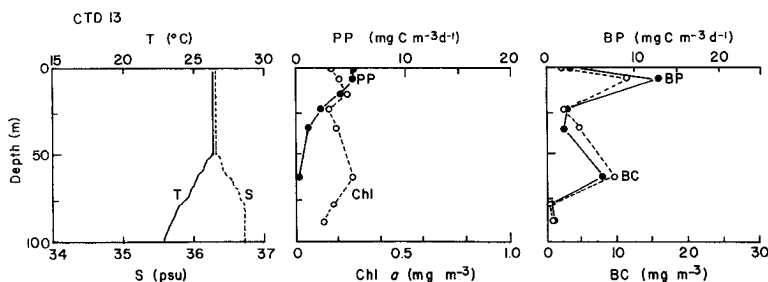
Figure 15. Temperature and salinity profiles (left panel) from CTD 13 in the Gulf Stream. Primary productivity rates and chlorophyll *a* profiles (mid panel) are taken from Niskin bottle casts, as are bacterial carbon biomass and productivity (right panel).

horizontal gradients in τ, the lateral boundaries were characterized by high gradients in $|d\tau/dx|$ (Fig. 14). The correspondence between high gradients in τ and high C_c is much clearer at this high resolution than in the complete transect. Low C_c values occurred in the intrusive features, again suggesting that small-scale mixing processes were concentrated in regions of strong property gradients. The *Tu* values reinforce the patterns observed in the complete transect with high values outlining the interface of the shallower Shelf water and deeper Gulf Stream features near -50 km (Fig. 14). The inclined region of low *Tu* values near -45 km marks the boundary between overlying warmer, saltier waters and fresher, cooler waters.

d. Plankton distributions

Plankton communities in the Gulf Stream were distinct from those in both streamers, which contained netplankton species and biomass levels typical of the Slope waters. At CTD 13 in the Gulf Stream the chlorophyll *a* concentrations were <0.1 mg m^{-3} throughout the 50 m-deep mixed layer (Fig. 15). Maximum pigment concentrations of 0.2 mg m^{-3} occurred in a subsurface layer near the thermocline. Photosynthetic rates were also relatively low, with maximum values of 0.5 mg C m^{-3} h^{-1} at the surface and an estimated daily productivity rate of 145 mg C m^{-2} d^{-1} Bacterial carbon biomass increased by an order of magnitude between the surface and the depth of the subsurface pigment maximum (Fig. 15). Carbon uptake rates for bacteria were quite variable with depth, ranging from 0.3 to >1 mg C m^{-3} d^{-1}, although the vertical distribution of bacterial carbon uptake paralleled that of bacterial biomass (Fig. 15).

As expected, the netphytoplankton abundance was relatively low in the oligotrophic Gulf Stream and species composition was diverse. Diatom abundance was <2 ml^{-1} in the mixed layer, with large centrics (*Hemiaulus* sp., *Rhizosolenia* spp.) and relatively few *Chaetoceros* spp. dominating the largest size fraction. Maximum diatom numbers were found in the thermocline where *Paralia, Ditylum* and *Coscino-*
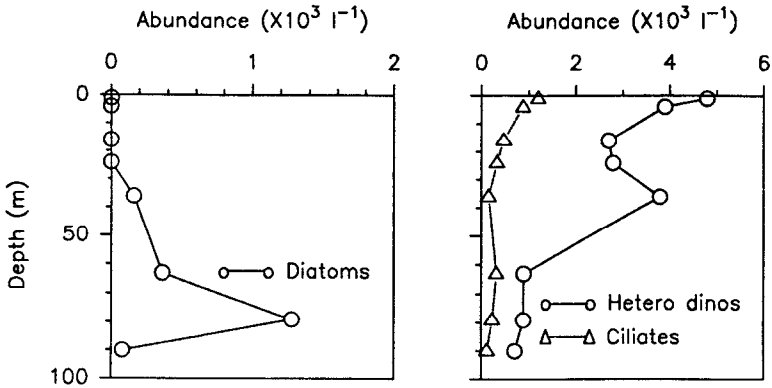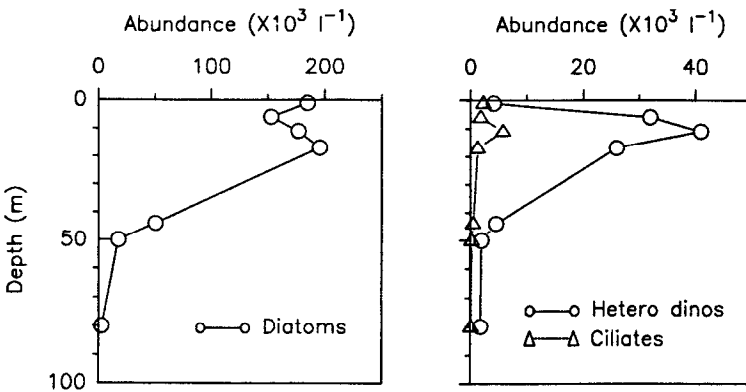
Figure 16. Vertical distribution of diatoms, heterotrophic dinoflagellates, and ciliates from whole water samples collected from Niskin bottles. Top: CTD 13 in the Gulf Stream; bottom: CTD 20 in the Gulf Stream streamer.

discus spp. dominated at abundances > 100 cells ml⁻¹. *Nitzschia delicatissima* was present only in the subsurface netplankton maximum, which was ≈ 10-m deeper than the subsurface pigment maximum (Fig. 15). The vertical distribution of heterotrophic microplankton in the Gulf Stream did not parallel that of pigment biomass. Instead, the highest microzooplankton abundances occurred near the surface maxima in both primary and bacterial productivity. Cell counts from the whole water samples indicated the near-surface maximum in microzooplankton was primarily composed of ciliates and heterotrophic dinoflagellates (Fig. 16). There was less vertical
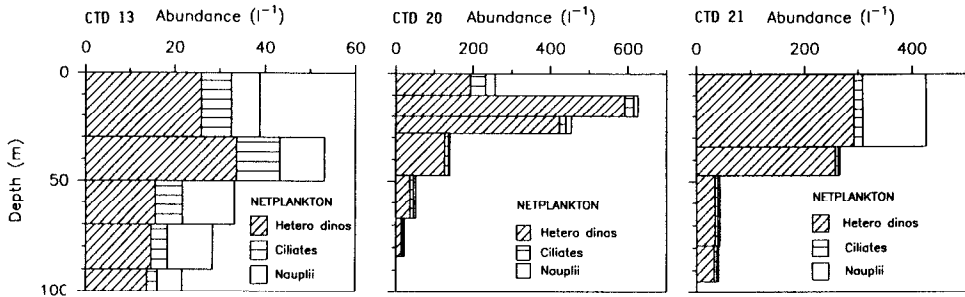
Figure 17. Abundances of netplankton (heterotrophic dinoflagellates, ciliates, copepod nau-
plii) from depth-integrated samples collected with the pump. Netplankton samples were
collected immediately after CTD 13 (Gulf Stream), CTD 20 (Gulf Stream streamer), and
CTD 21 (Shelf water streamer).

structure evident in the distribution of ciliates than in the other two microzooplank-
ton groups.

The vertical distribution of the net-microplankton sampled by the pump system
was similar to that of the microplankton fraction enumerated from whole water
samples (cf. Fig. 16, 17). The net-microplankton, however, were nearly 100-fold less
abundant than the microplankton. Depth-integrated samples from the plankton
pump suggest that the highest biomass interval of the net-microplankton may have
coincided with the subsurface pigment maximum at the base of the mixed layer.
Copepod nauplii exhibited less variation with depth than did the ciliates or heterotro-
phic dinoflagellates (Fig. 17).

Two stations were occupied on YD 283, the first characterized by a warm, salty,
surface layer and the second by a cooler, fresher mixed layer (Fig. 18). An SST image
taken 6 h before the first station (CTD 20) indicated the ship was at the southern
edge of the Gulf Stream streamer (Fig. 3d). A second SST image at 18:33 GMT was
partially obscured by clouds (not shown), but indicated that at CTD 21 the ship was
positioned in the Shelf water streamer. Surface properties at the two CTD stations
are consistent with this interpretation. The mixed layer at CTD 20 was relatively
shallow with a temperature of 24.5°C and salinity of 35.8 psu (Fig. 18, top). The SST
image taken just prior to CTD 20 indicated a surface temperature of $\approx 24°–25°C$ at
the center of the Gulf Stream streamer. The mixed layer in the Gulf Stream streamer
was $\approx 2°C$ cooler and 0.5 psu fresher than in the surface layer of CTD 13 in the Gulf
Stream. While the SST imagery indicated that the streamer originated from the Gulf
Stream, the hydrographic characteristics of the mixed layer show the feature had
cooled and freshened within five days. Several inversions in temperature and salinity
were seen at the base of the streamer (Fig. 18); these are consistent with the
interleaved warm/salty and cool/fresh layers in the Seasoar sections through this
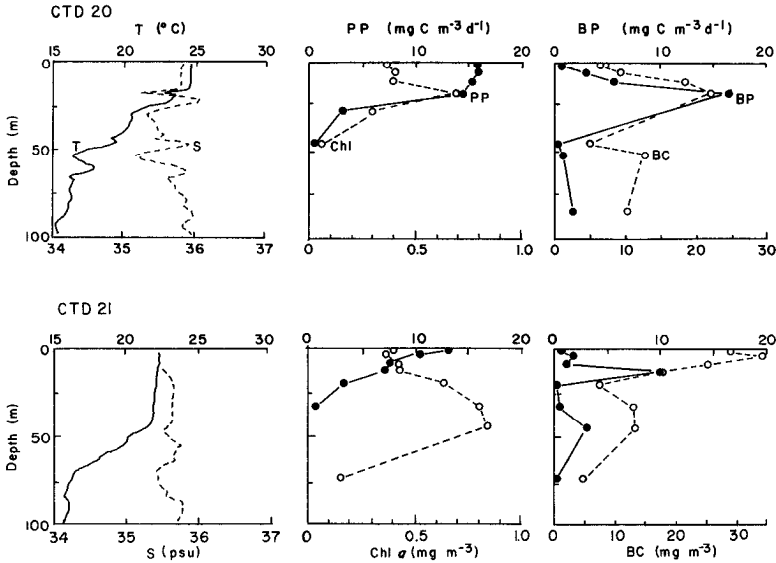region, and the variability evident in the ISF transect.

Figure 18. Same as Figure 15, but for CTD 20 in the Gulf Stream streamer and CTD 21 in the Shelf water streamer.

Nitrate concentrations ranged from 0.1 μM in the mixed layer of the Gulf Stream streamer to > 1 μM in the pycnocline. Chlorophyll *a* biomass in the surface layer was several-fold higher than in the Gulf Stream, with a subsurface maximum of 0.5 mg m^{-3} at the base of the mixed layer. The vertical distribution of pigment at the CTD stations parallels that in the fluorescence sections from the Seasoar, with both indicating maximum fluorescence near the pycnocline. Although the highest pigment concentrations in the streamer exceeded those in the source waters, the depth-integrated pigment biomass was similar (≈ 20 mg m^{-2}). Productivity rates in the streamer were also higher than in the Gulf Stream, exceeding 1.5 mg C m^{-3} h^{-1}, and the depth-integrated daily production estimate of 357 mgC m^{-2} d^{-1} was nearly 2-fold higher. Bacterial biomass and productivity rates in the surface layer of the streamer were also higher than in the Gulf Stream (Fig. 18). Bacteria cell carbon increased with depth to a maximum of 18 mg C m^{-3} at the base of the mixed layer and, as in the Gulf Stream, the vertical distribution of carbon fixation rates paralleled bacterial biomass. The highest bacterial productivity rates (18 mg C m^{-3} d^{-1}) occurred near the subsurface chlorophyll *a* maximum (Fig. 18). Below the pycnocline the distribution of bacterial biomass was low and quite variable.

The species composition of the diatom community was rather uniform throughout the water column at CTD 20, and the relative proportion of species did not vary much with depth. *Skeletonema costatum* was the most abundant diatom throughout the upper 80 m with cell densities > 10^5 l^{-1}. Three other chain-forming centrics, *Nitzschia delicatissima, Leptocylindrus danicus* and *L. minimus,* and several species of

Rhizosolenia and *Chaetoceros,* comprised the remaining dominant netphytoplankton in the upper 80 m. While *Skeletonema* numerically dominated the larger photoauto-trophs, several *Rhizosolenia* species composed the largest fraction of diatom biomass at all depths (E. Lessard, unpub. data). Total heterotrophic microplankton numbers were also higher in the streamer than in the Gulf Stream, although individual taxonomic groups varied in abundance through the water column. Maximum abun-dances of heterotrophic dinoflagellates and ciliates were found near the pycnocline, at 20 m (Fig. 16). The larger net-microplankton exhibited similar patterns with the abundances of all three taxonomic groups several-fold higher than in the Gulf Stream (Figs. 17).

The Shelf water streamer sampled at CTD 21 was characterized by a cooler (22.5°C) and fresher (35.4 psu) surface layer than in the streamer which originated from the Gulf Stream. A weak halocline was present at 10 m (Fig. 18). In contrast to the other streamer, nitrate concentrations were <0.1 μM throughout the mixed layer. Chlorophyll *a* concentrations increased with depth to a subsurface maximum of 0.8 mg m^{-3} near the pycnocline (Fig. 18). These values are typical of the Slope water in the fall (Cox *et al.,* 1982). The depth-integrated chlorophyll *a* biomass for the euphotic zone (42.9 mg m^{-2}) was 2-fold greater than that at CTD 20. Productivity rates, in contrast, were slightly lower than in the other streamer, and comparable to those observed in the Gulf Stream. The low nitrate concentrations, high pigment biomass, and relatively low productivity rates suggest that the phytoplankton biomass in the Shelf water streamer may have been nutrient-limited. The vertical distribution of bacterial productivity paralleled that of bacterial C biomass in the mixed layer of the Shelf water streamer (Fig. 18). While surface bacterial biomass was higher than in the Gulf Stream streamer, the bacterial C biomass at depth was similar (≈ 10 mg C m^{-3}). The highest bacterial productivity rates of 10 mg C m^{-3} d^{-1} coincided with the weak halocline at 10 m.

Although no quantitative cell counts were available from whole water samples at CTD 21, the phytoplankton taxa recorded from the depth-integrated pump samples showed that similar diatom genera dominated the netplankton community in both streamers. The netplankton community in the upper 75 m of the Shelf water streamer was dominated by *Skeletonema costatum, Chaetoceros* spp., *Leptocylindrus danicus, L. minimus* and *Nitzschia delicatissima* (E. Lessard, unpub. data). Larger *Rhizosolenia spp.* accounted for the major fraction of cellular biovolume. Below the mixed layer the cell abundances decreased 100-fold. In the deepest interval sampled, between 75 to 100 m, several large genera were found which were otherwise only seen in the Gulf Stream, such as *Paralia.* The ciliates, heterotrophic dinoflagellates and nauplii enumerated from the pump samples revealed that the highest abun-dances occurred in the upper 30 m of the mixed layer (Fig. 17). The maximum net-microplankton abundance in the Shelf water streamer was half that in the Gulf Stream streamer. There was little variability in the vertical distribution of the

microzooplankton below 70 m, for at these depths the abundance was less than in the Gulf Stream.

4. Discussion

a. The cyclonic eddy

The high-salinity filament of Gulf Stream water which defined the cyclonic eddy possessed a thermal signature similar to the frontal eddies of the SAB. Both eddies are seen in SST imagery as a warm surface filament which is several km wide and tens-to-hundreds of km long. South of Cape Hatteras the frontal eddies form along the shoreward edge of current meanders and lengthen as the amplitude of meanders increase downstream (Lee *et al.*, 1991). The typical lifetime of a frontal eddy is one-to-two weeks (Lee *et al.*, 1981). Several characteristics of the cyclonic eddy formed east of Cape Hatteras, however, were distinct from frontal eddies. First, the cyclonic eddy did not propagate downstream as an entity; only the point of attachment to the Stream front propagated to the east. Second, the surface signature of the cyclonic eddy was evident in SST imagery for only three days. Two other eddies which formed farther south disappeared from the SST imagery within 24 hours. The lifetime of cyclonic eddies formed east of Cape Hatteras may therefore be shorter than those of frontal eddies in the SAB. This may reflect the interaction of the Gulf Stream with warm-core rings in the Slope water, or dynamical processes associated with the increasing amplitude of meanders downstream.

Frontal eddies in the SAB are composed of surface Gulf Stream filaments which overlie a 'dome' of cooler subsurface waters upwelled from the nutrient-rich waters of the upper pycnocline. Circulation patterns in the surface filaments of frontal eddies have been interpreted as either cyclonic, with southerly flow over the entire width of the filament (Lee *et al.*, 1981), or anticyclonic, with horizontal shear across the filament (Chew, 1981; Pietrafesa, 1983). Perhaps both flow patterns exist, depending upon local topography, wind forcing, or which part of the feature is being examined. However, the flow pattern within the surface filament of the cyclonic eddy was cyclonic over the entire width of the filament. This conclusion is supported by the surface velocity vectors, the slope of the isohalines in the salinity section, and the elongation of the warm filament in successive SST images.

The development of the cold dome in frontal eddies supports enhanced nutrient concentrations within the surface waters of the SAB. Narrow ($L \approx 10$ km), elongate ($L \approx 100$ km) bands of chlorophyll typically develop shoreward of the Gulf Stream front in association with frontal eddies (Yoder *et al.*, 1981; McClain *et al.*, 1984). These pigment maxima are the main source of spatial variability in the surface chlorophyll distribution on the outer shelf of the Bight (Yoder *et al.*, 1987). Although there were no pigment sections obtained from the Seasoar transects which crossed the cyclonic eddy, it is likely that this feature did not contain a localized pigment maximum. At the center of the cyclonic eddy surveyed in SS 21, the isopycnal

surfaces of the upper pycnocline shoaled to depths comparable to those farther downstream, where no cyclonic circulation was evident (see Lillibridge *et al.,* 1990). This implies little 'doming' of the pycnocline in the center of this feature. Churchill and Cornillon (1991) have similarly concluded that downstream of Cape Hatteras the smaller eddies present along the Gulf Stream front may be distinct from frontal eddies in the SAB, and likely have less of an impact on local productivity gradients. This limited number of observations suggest that cyclonic eddies formed downstream of Cape Hatteras are fundamentally different in structure from the frontal eddies of the SAB.

b. Mixing processes

The conductivity and temperature sensors on the Seasoar yield three indices which provide insight into the location and nature of mixing processes. The CTD recorded variability in the conductivity signal at scales of 10 cm to 1 m, but did not resolve the variability on the cm scale (the length scale of double diffusive processes). Nevertheless, the conductivity Cox numbers provide a useful measure of microstructure activity (Georgi *et al.,* 1983). Where diapycnal mixing occurs across isopycnal surfaces, then high Cox numbers are expected in regions of salt fingering (very low *Tu*) or diffusive convection (very high *Tu*). Additionally, if the mixing processes mainly occurred along isopycnal surfaces, then high conductivity Cox numbers should be concentrated at the vertical property fronts, with large horizontal gradients in tau. It is assumed that mixing proceeds at the boundaries of the layered intrusions in these property fronts. [The actual mixing process is likely diapycnal, with salt fingers forming where warm, salty waters overlie cold, fresh waters (low Turner angle), and diffusive convection in the opposite case (high Turner angle).]

High conductivity Cox numbers were occasionally, but not always, associated with low and high Turner angles. This occurred mainly at the lateral boundaries of the Gulf Stream, warm-core ring, and streamers. The pattern suggests that salt fingering and diffusive convection were the most significant mechanisms contributing to mixing in the strongest property fronts. Similar patterns were found farther upstream, at the periphery of Ford Water features (Lillibridge *et al.,* 1990). Schmitt *et al.* (1986) also reported a fair correspondence between high conductivity Cox numbers and R_p, the density ratio, which was interpreted as evidence of salt fingering activity at the edge of a warm-core ring. Georgi and Schmitt (1983) similarly found a close correspondence between conductivity Cox numbers and an optical index of microstructure activity in vertical profiles near the property front of the North Atlantic Current.

The process by which the intrusive features were generated was first described by Ruddick and Turner (1979); Schmitt (1994) has reviewed subsequent observations. Contrasting water masses may penetrate in the form of long, thin intrusions which are driven by salt fingering between warm, salty intrusions and cold, fresh intrusions, and by diffusive layering in the opposite case. An estimate of the vertical scale of the

intrusive features can be derived from:

$$H = 3/2 \, (1 - n) \, \beta \Delta S \, [1/\rho_o \cdot d\rho/dz]^{-1} \qquad (3)$$

where H is the thickness in m, n is the density ratio, and $\beta \Delta S$ is product of the haline expansion coefficient times the salinity gradient (Ruddick and Turner, 1979). When this formula is applied to conditions present in the middle of SS 26 (Fig. 14), the largest uncertainty is in the estimate of ΔS. Where the salinity minimum of 34.4 psu borders a salinity maximum of 36.2 psu, at ≈ -46 km, the maximum horizontal salinity gradient is 1.8 psu. Utilizing $7.7 \cdot 10^{-4}$ for β, $10^{-3}/30$ m for $1/\rho \cdot d\rho/ dz$, and $n = 0.56$ for salt fingering, the thickness of an intrusive feature (H) is estimated at 27 m. This value agrees with the thickness of the intrusive features in the transects, with observations from other regions (e.g., Voorhis et al., 1976), and with estimates derived from more rigorous formulations (Yoshida et al., 1991).

The distributions of the various mixing indices presents an enigma: if double diffusive processes contribute to the development of intrusions, then high conductivity Cox numbers should be observed in conjunction with high or low Turner angles. In the transects, however, high Cox numbers were most frequently correlated with high horizontal gradients in tau (Fig. 14). There can be no direct correspondence between the conductivity Cox number and the horizontal gradient in τ, since each index was computed at different horizontal scales. The conductivity Cox numbers span horizontal scales of 0.1 m to 3.5 m, while $|d\tau/dx|$ was computed as the difference between successive SeaSoar profiles, corresponding to a horizontal scale of 800 to 1000 m. One potential explanation for this apparent discrepancy is that the Turner angle was estimated for a larger vertical scale than was the estimate of microstructure activity (<1 m).

An alternative explanation is that while low Turner angles are a sufficient condition for salt fingering, the development may be inhibited in regions of high vertical shear, if shear suppresses the growth of salt fingers. This factor could contribute to the lack of a strong and consistent correlation between low Turner angles and high Cox numbers at the Gulf Stream front. High Cox numbers can also arise in response to shear flow instabilities independent of the Turner angle. However, prior observations with the Seasoar in Ford Water features suggest that vertical shear is not a major factor contributing to mixing in the Gulf Stream front. Although vertical shear was not measured in SS 21 to 32, Lillibridge et al. (1990) estimated the gradient Richardson number (R_i) farther upstream. The values along the edge of the Stream were typically 0.7 and larger, above the limit necessary for instability ($R_i \leq 0.25$). Evans (1982) also concluded minimal shear flow instability exists in the Gulf Stream front, based on observations with the microstructure profiler YVETTE. Thus mixing appears to have mainly occurred by double diffusive processes which were concentrated in the property fronts.

c. Plankton distributions

The fluorescence patterns from the Seasoar transects indicates that stirring mechanisms can affect the spatial distribution of plankton biomass within the Slope water. This was evident in a localized fluorescence minimum associated with a Shelf water streamer at the depth of the subsurface pigment maximum in the Slope water and in the local maximum in the Ford Water. Shelf water streamers have been previously observed to advect relatively high concentrations of pigment biomass across the Shelf/Slope front. A cool shelf water streamer sampled south of Georges Bank contained a localized subsurface chlorophyll *a* maximum in August, 1984 (Yentsch and Phinney, 1986). Shelf water streamers are also capable of exporting considerable quantities of suspended particulate matter from the Shelf (Joyce *et al.,* 1992) and fish larvae (Flierl and Wroblewski, 1985). Thus the minimum in fluorescence in the Shelf water streamer in SS 26 contrasts with high pigment and particulate loads typically found in streamers close to the Shelf/Slope front. This pattern suggests that pigment biomass in the streamer may have decreased with time as the feature was advected about the ring.

A curious aspect of the Gulf Stream and Shelf streamers was that the species composition of the netplankton community in both was similar to the Slope water. Additionally, the diatom community in a surface Ford Water feature sampled at 36.5N prior to this study was also dominated by *Skeletonema costatum,* while a subsurface Ford Water filament was dominated by *Nitzschia delicatissima* and *Rhizosolenia* spp. (Lillibridge *et al.,* 1990). It had been previously hypothesized that the diatom composition of Ford Water may reflect the populations at the Shelf water source. However, these same species also dominated the autotrophic netplankton community in streamers which originated from the Shelf water and the Gulf Stream. The observations therefore suggest that the netplankton were seeded into the various features from a common source, the contiguous Slope water.

Small-scale mixing processes at the boundaries of the streamers are one mechanism by which microplankton could have been introduced into the features from the Slope water. Salt fingers can enhance the flux of nutrients across property fronts (Hamilton *et al.,* 1989), and contribute to the development of optimal photoenvironments (Lewis *et al.,* 1984). Recent advances in sampling technology have documented the occurrence of concentrated plankton biomass in layers of microscale dimensions (e.g., Cowles *et al.,* 1993). Double diffusive processes at the property fronts may, therefore, be a mechanism by which similar diatom species were mixed into streamers originating from the Gulf Stream and Shelf water. The streamer derived from the Gulf Stream had obviously mixed with the surrounding Slope waters, since the salinity and temperature of the feature were less than that of the Gulf Stream source waters. The mixing of Slope waters would also 'seed' the streamer with Slope water phytoplankton species. Nutrient influx at the base of the streamer may also have been enhanced by mixing processes at the pycnocline. It is

important to distinguish that the mixing processes would not concentrate Slope water species in the streamer. Once introduced, the allochthonous species would have to rapidly reproduce and maintain a net growth rate sufficient to overcome losses in order to attain the observed cell densities.

The similarity in netplankton species composition in both the Gulf Stream and Shelf water streamer, as well as Ford Water, may therefore reflect the mixing of Slope water into these features. The diatom species presumably have high growth rates under the prevailing environmental conditions, and could likely rapidly dominate the netplankton community. This hypothesis implies that the community in streamers and Ford water features evolve at a rate which is faster than that at which the physical characteristics change, such as SST signatures. This rapid evolution of the biological characteristics of streamers is analogous to the changes observed in plankton communities within warm-core rings (Olson, 1991). The dynamics of rings lead to enhanced productivity and changes in both species composition and biomass before the physical characteristics of the ring decay. Clearly the dynamics of plankton communities in the surface waters near the Gulf Stream front are influenced by a variety of physical processes, ranging from stirring on the mesoscale to mixing processes on the microscale.

d. Summary

Property sections mapped by the Seasoar reveal that streamers and intrusive features are commonly generated by eddies near the Gulf Stream front. Although two eddies differed in diameter by nearly an order of magnitude, both had entrained filaments of Gulf Stream or Shelf water of similar dimensions: 100 km in length, 10 km in width, and 10's of meters thick. The filaments and narrower intrusive features were bordered by sharp horizontal and vertical gradients in temperature and salinity which were active sites of mixing. This 'cascade of scales' in the processes which mediate the exchange of Gulf Stream water across the front reveals that eddies not only stir the contiguous Slope and Gulf Stream waters, but also contribute to the mixing of contrasting water types at the property fronts. These processes also can directly influence the distribution and productivity of the plankton community adjacent to the Gulf Stream front.

Journal of Marine Research [52, 5

REFERENCES

Anonymous. 1985. Oceanographic Monthly Summary. Volume 5. National Oceanic and Atmospheric Administration, National Ocean Service.

—— 1986. Studies of mixing and stirring along the northern Gulf Stream edge. Institute of Geophysics Technical Report 65, University of Bergen, Bergen, Norway, 120 pp.

Børsheim, K. Y. 1990. Bacterial biomass and production rates in the Gulf Stream front regions. Deep-Sea Res., *37*, 1297–1309.

Bower, A. S. 1991. A simple kinematic mechanism for mixing fluid parcels across a meandering jet. The Synoptician, *2*, 1–4.

Bower, A. S., R. O'Gara and T. Rossby. 1986. RAFOS pilot studies in the Gulf Stream, 1984–1985. Graduate School of Oceanography, Univ. of R.I. Technical Report 86-7, Narragansett, R.I. 110 pp.

Bower, A. S. and T. Rossby. 1989. Evidence of cross-frontal exchange processes in the Gulf Stream based on isopycnal RAFOS float data. J. Phys. Oceanogr., *19*, 1177–1190.

Bower, A. S., T. Rossby and J. L. Lillibridge, Ill. 1985. The Gulf Stream—Barrier or blender? J. Phys. Oceanogr., *15*, 24–32.

Chew, F. 1981. Shingles, spin-off eddies, and an hypothesis. Deep-Sea Res., *28*, 379–391.

Churchill, J. H. and P. C. Cornillon. 1991. Water discharged from the Gulf Stream north of Cape Hatteras. J. Geophys. Res., *96*, 22,217–22,243.

Cowles, T. J., R. A. Desiderio and S. Neuer. 1993. *In situ* characterization of phytoplankton from vertical profiles of fluorescence emission spectra. Mar. Biol., *115*, 217–222.

Cox, J. L., P. H. Wiebe, P. Ortner and S. Boyd. 1982. Seasonal development of subsurface chlorophyll maxima in slope water and northern Sargasso Sea of the northwestern Atlantic Ocean. Biol. Oceanogr., *1*, 271–285.

Dewar, W. K. and G. R. Flierl. 1985. Particle trajectories and simple models of transport in coherent vortices. Dyn. Atmos. Oceans, *9*, 215–252.

Dutkiewicz, S., A. Griffa and D. B. Olson. 1993. Particle diffusion in a meandering jet. J. Geophys. Res., *98*, 16,487–16,500.

Evans, D. L. 1982. Observations of small-scale shear and density structure in the ocean. Deep-Sea Res., *29*, 581–595.

Flierl, G. R. and J. S. Wroblewski. 1985. The possible influence of warm-core Gulf Stream rings upon shelf water larval fish distribution. Fish. Bull., *83*, 313–330.

Ford, W. L., J. R. Longard and R. E. Banks. 1952. On the nature, occurrence, and origin of cold low salinity water along the edge of the Gulf Stream. J. Mar. Res., *11*, 281–293.

Garrett, C. 1983. On the initial streakiness of a dispersing tracer in two- and three-dimensional turbulence. Dyn. Atm. Oceans, *7*, 265–277.

Georgi, D. T., R. C. Millard and R. W. Schmitt. 1983. Conductivity microstructure measurements with a CTD, *in* Third Working Symposium on Oceanographic Data Systems, IEEE Computer Society and Woods Hole Oceanographic Institution, C. D. Tollios, M. K. McElroy, and J. Syck, eds., symposium proceedings, Woods Hole, MA, 5–14.

Georgi, D. T. and R. W. Schmitt. 1983. Fine and microstructure observations on a hydrographic section from the Azores to the Flemish Cap. J. Phys. Oceanogr., *13*, 632–647.

Hamilton, J. M., M. R. Lewis and B. R. Ruddick. 1989. Vertical fluxes of nitrate associated with salt fingers in the world's oceans. J. Geophys. Res., *94*, 2137–2145.

Jackett, D. R. and T. J. McDougall. 1985. An oceanographic variable for the characterization of intrusions and water masses. Deep-Sea Res., *32*, 1195–1207.

Joyce, T. M., J. K. B. Bishop and O. B. Brown. 1992. Observations of offshore shelf-water transport induced by a warm-core ring. Deep-Sea Res., *39*, S97–S113.

Williams, A. J. 1981. The role of double diffusion in a Gulf Stream frontal intrusion. J. Geophys. Res., *86*, 1917–1928.

Lee, T. N., L. P. Atkinson and R. V. Legeckis. 1981. Detailed observations of a Gulf Stream spin-off eddy on the Georgia continental shelf. Deep-Sea Res., *28*, 347–378.

Lee, T. N., J. A. Yoder and L. P. Atkinson. 1991. Gulf Stream frontal eddy influence on productivity of the southeast U.S. continental shelf. J. Geophys. Res., *96*, 22,191–22,205.

Lewis, M. R., E. P. W. Horne, J. J. Cullen, N. S. Oakey and T. Platt. 1984. Turbulent motions may control phytoplankton photosynthesis in the upper ocean. Nature, *314*, 49–50.

Lillibridge, J. L., III. 1989. Computing the seawater expansion coefficients directly from the 1980 equation of state. J. Atmosph. Oceanic Tech., *6*, 59–66.

Lillibridge, J. L., III, G. Hitchcock, T. Rossby, E. Lessard, M. Mork and L. Golmen. 1990. Entrainment and mixing of shelf/slope waters in the nearsurface Gulf Stream. J. Geophys. Res., *95*, 13,065–13,087.

McClain, C. R., L. J. Pietrafesa and J. A. Yoder. 1984. Observations of Gulf Stream induced and wind driven upwelling in the Georgia Bight using ocean color and infrared imagery. J. Geophys. Res., *89*, 3705–3723.

Nof, D. 1986. The collision between the Gulf Stream and warm-core rings. Deep-Sea Res., *33*, 359–378.

Oakey, N. S. and J. A. Elliott. 1977. Vertical temperature gradient across the Gulf Stream. J. Geophys. Res., *82*, 1369–1380.

Olson, D. B. 1991. Rings in the ocean. Annu. Rev. Earth Planet. Sci., *19*, 283–311.

Owen, J. R. 1989. Microscale and finescale variations of small plankton in coastal and pelagic environments. J. Mar. Res., *47*, 197–240.

Pietrafesa, L. J. 1983. Survey of a Gulf Stream frontal filament. Geophys. Res. Lett, *10*, 203–206.

Pollard, R. 1986. Frontal surveys with a towed profiling conductivity/temperature/depth measurement package (SeaSoar). Nature, *323*, 433–434.

Rossby, H. T., D. Dorson and J. Fontaine. 1986. The RAFOS system. J. Atmos. Oceanic Tech., *3*, 672–679.

Rossby, H. T., E. R. Levine and D. N. Connors. 1985. The isopycnal Swallow float—A simple device for tracking water parcels in the ocean. Prog. Oceanogr., *14*, 511–525.

Ruddick, B. R. 1983. A practical indicator of the stability of the water column to double-diffusive activity. Deep-Sea Res., *30*, 1105–1107.

Ruddick, B. R. and J. S. Turner. 1979. The vertical length scale of double-diffusive intrusions. Deep-Sea Res., *26*, 903–913.

Schmitt, R. W. 1994. Double diffusion in oceanography. Ann. Rev. Fluid Mech., *26*, 255–285.

Schmitt, R. W. and D. T. Georgi. 1982. Finestructure and microstructure in the North Atlantic Current. J. Mar. Res., *40*, (Suppl.), 659–705.

Schmitt, R. W., R. G. Lueck and T. M. Joyce. 1986. Fine- and microstructure at the edge of a warm-core ring. Deep-Sea Res., *33*, 1665–1689.

Tang, C. L., A. S. Bennett and D. J. Lawrence. 1985. Thermohaline intrusions in the frontal zones of a warm-core ring observed by Batfish. J. Geophys. Res., *90*, 8928–8942.

Veronis, G. 1972. On properties of seawater defined by temperature, salinity and pressure. J. Mar. Res., *30*, 227–255.

Von Arx, W. S., D. Bumpus and W. S. Richardson. 1955. On the fine structure of the Gulf Stream front. Deep-Sea Res., *3*, 46–65.

Voorhis, A. D., D. C. Webb and R. C. Millard. 1976. Current structure and mixing in the shelf/slope water front south of New England. J. Geophys. Res., *81*, 3695–3708.

Washburn, L. and R. H. Käse. 1987. Double diffusion and the distribution of the density ratio in the Mediterranean waterfront southeast of the Azores. J. Phys. Oceanogr., *17*, 12–25.

Williams, A. J. 1981. The role of double diffusion in a Gulf Stream frontal intrusion. J. Geophys. Res., *86*, 1917–1928.

Wishner, K. F., and S. K. Allison. 1986. The distribution and abundance of copepods in relation to the physical structure of the Gulf Stream. Deep-Sea Res., *33*, 705–731.

Yentsch, C. S. and D. A. Phinney. 1986. The role of streamers associated with mesoscale eddies in the transport of biological substances between Slope and ocean waters, *in* Marine Interfaces Hydrodynamics, Elsevier Oceanography Series, *42*, Elsevier, New York, 153–163.

Yoder, J. A., L. P. Atkinson, T. N. Lee, H. H. Kim and C. R. McClain. 1981. Role of Gulf Stream frontal eddies in forming phytoplankton patches on the outer southeastern shelf. Limnol. Oceanogr., *25*, 1103–1110.

Yoder, J. A., C. R. McClain, J. O. Blanton and L.-Y. Oey. 1987. Spatial scales in CZCS-chlorophyll imagery of the southeastern U.S. continental shelf. Limnol. Oceanogr., *32*, 929–941.

Yoshida, J., H. Nagashima and H. Niino. 1991. The behavior of double diffusive intrusions in a rotating system. Woods Hole Oceanogr. Inst. Tech. Report, *WHOI-91-20*, 183–191.